2013

Squaraine dyes for two-photon fluorescence bioimaging applications

Maria Colon Gomez
University of Central Florida

SQUARAINE DYES FOR TWO-PHOTON FLUORESCENCE BIOIMAGING APPLICATIONS

by

MARIA YEZABEL COLÓN GOMEZ

A thesis submitted in partial fulfillment of the requirements
for the Honors in the Major Program in Chemistry
in the College of Sciences
and in The Burnett Honors College
at the University of Central Florida
Orlando, Florida

Spring Term 2013

Thesis Chair: Dr. Kevin D. Belfield

ABSTRACT

Near-infrared emitting squaraine dyes are promising candidates for bioimaging applications. Two-photon fluorescence microscopy (2PFM) imaging is a powerful tool being used for studying biological function since it produces 3D images with minimal damage to cells and lower fluorophore photobleaching. The fluorescence wavelength of squaraine dyes normally falls in the near infrared region, providing deeper penetration through biological samples such as thick tissue sections. Squaraine dyes that could work for imaging cells and tissues for 2PFM imaging were synthesized and underwent comprehensive photophysical characterization, such as UV-Vis absorption, fluorescence, and anisotropy. The squaraine dyes were tested for cell toxicity to determine the concentration at which the cells should be incubated with the dye for 2PFM. In addition, the squaraine dyes were incubated with cancer cells to evaluate their utility in the bioimaging process. The squaraine dye that is not soluble in water can be incorporated in silica nanoparticles or micelles to facilitate dispersal in water for evaluation of its use as a probe. The prospective squaraine dyes can be used in cells and tissues for imaging that can then be analyzed to ascertain its use as a probe for biomedical applications, such as early cancer detection.

To all the persons that help me reach this goal and to the people that have been affected with cancer; hope this material is one step closer to help those that are still affected by it.

ACKNOWLEDGEMENTS

An undertaking of this magnitude is not possible without the assistance of several important individuals. I would like to express my deepest appreciation to my advisors Dr. Kevin D. Belfield and Dr. Sheng Yao, who has provided me with a tremendous amount of guidance and support. I am privileged to have been accepted to the research group to work alongside great faculty members and the students that are part of this group. I also want to thank my committee members Dr. Andrew Frazer and Dr. Aristide Dogariu. In addition, I want to thank the members of the research group that collaborated and helped in the completion this project, especially Dr. Alma Morales, Xiling Yue, Bosung Kim, Rosmery Victoria and Haffeez Haniff.

TABLE OF CONTENTS

LIST OF FIGURES

LIST OF TABLES

CHAPTER 1: INTRODUCTION

The second leading cause of death in the United States is cancer (25% of deaths are due to cancer).[1] What is cancer? "Cancer is a group of diseases characterized by uncontrolled growth and spread of abnormal cells."[1] There are many different ways in which a person can be affected with cancer. They can acquire cancer from environmental factors, such as smoking or radiation, and they can also acquire cancer by genetic factors such as inheritance of abnormal genes.[1] In either case, there should be a way to prevent the population from acquiring cancer. Prevention can be accessed by control of certain physical behaviors or activities and/or by early diagnosis and treatment. As show in **Figure 1**, the earlier the detection of cancer, the higher the rate of survival for an individual that has cancer.

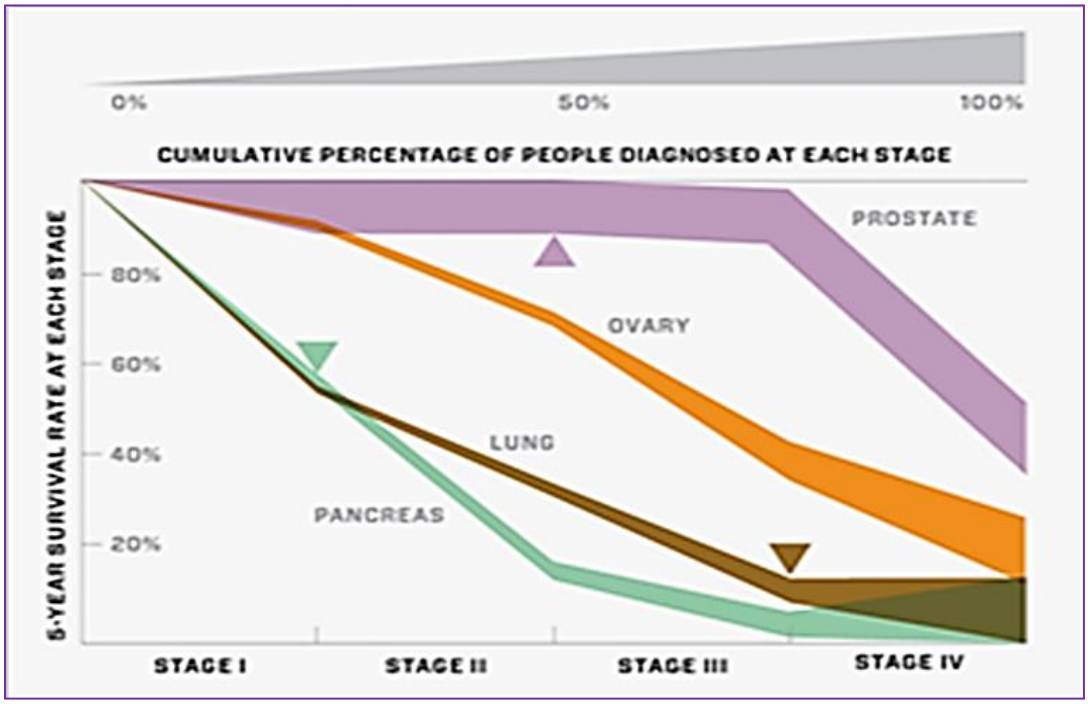

Figure 1. The correlation between rate of survival, diagnosis at different stages and data of the percentage of the population that are detected with cancer at different stages.[2]

Therefore, this fact demonstrates that early detection is critical for most cancers, yet less than one percent of government funding is spent on early detection research and development. The synthesis of near-infrared dyes that can potentially be used as probes in the applications of early cancer detection is reported in this thesis. Near-infrared dyes are fluorophores that can be useful for various biosensor applications. A fluorophore is a chemical compound that can re-emit light upon light excitation or in other words a molecule that fluoresces, such as a squaraine dye. These dyes have specific advantages that are helpful when dealing with biological media.[3] For instance, the dyes are used for tissue absorption, scattering, and autofluorescence in cells.[3] Squaraine dyes are promising candidates for bioimaging applications. They have high two photon cross-section [4] and emit at near infrared, the region where there is an optical window for biological samples. As shown in **Figure 2**, most biological samples have absorption in the visible region, but a number of biological materials have high transparency in the near-infrared region.[5]

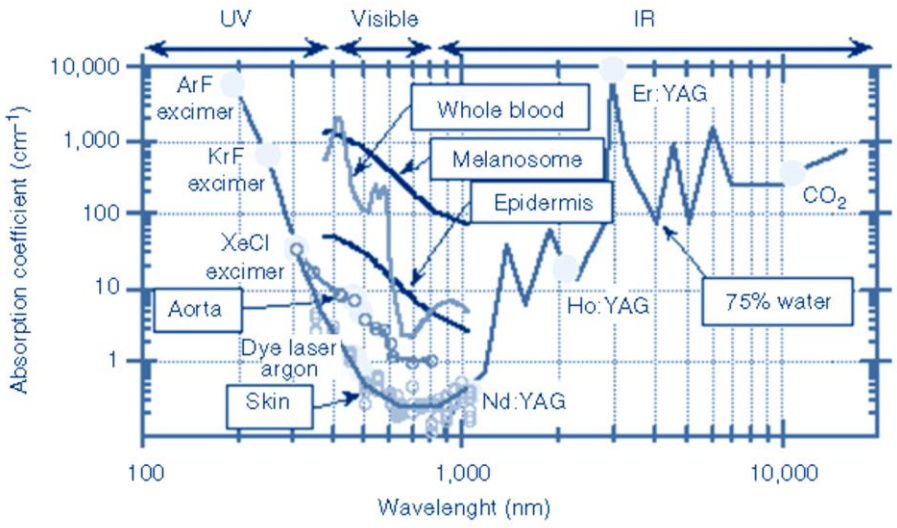

Figure 2. Primary absorption spectra of biological tissues along with their absorption coefficients at some AQ5 common laser wavelengths.[6]

Fluorescence is the result of the molecule or fluorophore undergoing a three stage process of excitation, internal conversion, and emission. These processes can be explained using the Jablonski diagrams, as shown in **Figure 3**.

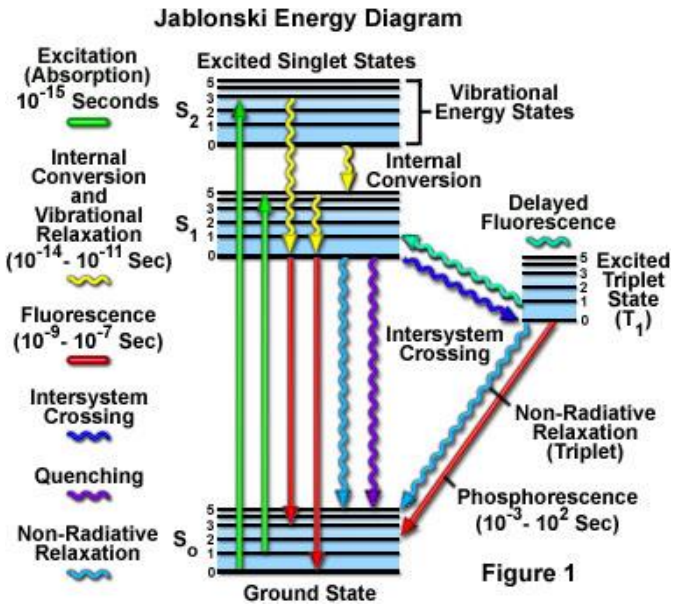

Figure 3. A Jablonski Diagram.[7]

When a molecule is electronically excited and a chemical reaction does not occur, the excess energy absorbed by the excited electron must be dissipated. This process could occur through vibrational relaxation, where the energy is dissipated to the surroundings or to the solvent in the form of heat; hence no emission occurs. This is considered a non-radiative transition from an excited to a more stable ground state. Non-radiative transitions from an excited state to the ground state occur relatively quickly, from 10^{-12} to 10^{-10} seconds.[8] It is also possible that a radiative transition may occur to dissipate this energy; one such transition is called phosphorescence. Phosphorescence occurs when an electron is promoted to an excited vibrational state and through internal conversion and vibrational relaxation, the electron reaches

the lowest vibrational singlet state and then undergoes an intersystem crossing, where the spin of the electron undergoes a change in direction or enters a state of forbidden spin-the triplet state. The energy of the triplet vibrational state is closer in energy to the ground state than the singlet state, because now the ground state electron and the excited electron have the same spin and thus, less energy is required to keep them apart. This electron undergoes vibrational relaxation until the lowest vibrational triplet state is achieved. The electron, with its remaining energy, emits a photon, this is called phosphorescence, with a life time of 10^{-3} to 10^{2} seconds.[8] This phenomenon requires more time than non-radiative transitions and fluorescence process. In addition, the electron may dissipate its excess energy through a radiative transition called fluorescence. Fluorescence occurs in a similar fashion to phosphorescence, with a couple of major differences. First, the relative occurrence time is shorter than phosphorescence, yet it is longer lived than non-radiative decay, with a time range of 10^{-9} to 10^{-7} seconds.[8] Second, the spin of the electron is maintained, but an intersystem crossing does not occur. This electron undergoes vibrational relaxation until the lowest vibrational singlet state is achieved. A photon lower in energy than the incident energy donating photon is released as it returns to the ground state. Two-photon excitation is the fluorescence process in which a fluorophore is excited from electronic ground state to an excited state by the simultaneous absorption of two long wavelength photons. Two-photon excited fluorescence differs from single photon excited fluorescence with regard to the excitation stage of the fluorescence process.[9] In the two-photon excitation process, the fluorophore achieves the transition from its ground state (S_0) to an excited state (S_n) by the near-simultaneous (~10^{-16}s) absorption of two photons.[9] "One photon excites the fluorophore to a 'virtual' intermediate state while the second photon further excites the fluorophore to the

excited state."[9] The wavelengths of the two-photon are roughly equal. The energies of the two-photon are almost half of the energy required in a one-photon excitation process. In the process two photons are required for each excitation event, therefore the probability of a fluorophore absorbing a photon pair is proportional to the square of the excitation intensity.[9] Thus, a high density of photons must be at the focal point for a reaction to happen between the two photons and the fluorophore. Beyond the focal point of a laser or microscope, the probabilities of two-photon absorption are tremendously low. The comparison between one-photon and two-photon excitation is shown in **Figure** 4.

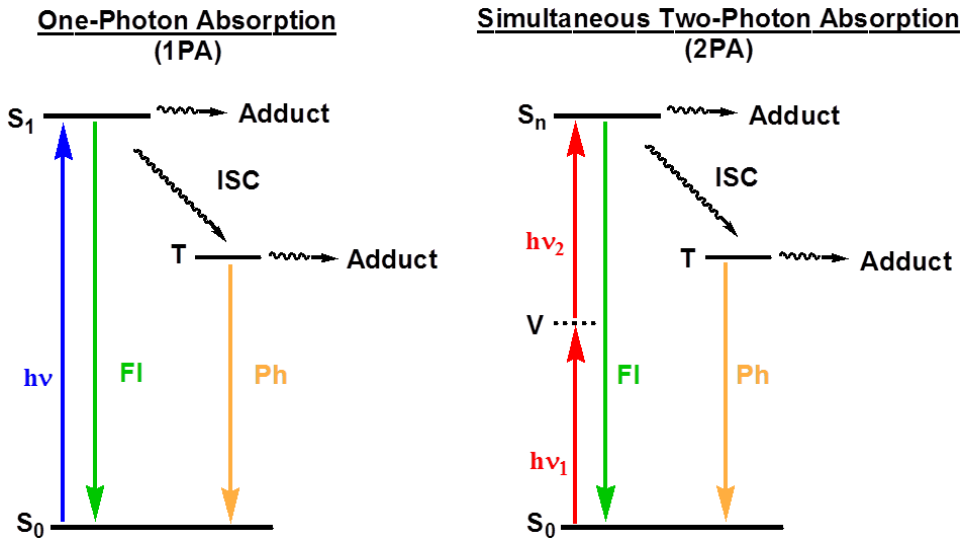

Figure 4. Simplified Jablonski energy level diagrams for comparison of single and two-photon absorption. Excitation of a molecule from the ground state (S_0) to an excited state (S_1) can occur through one-photon absorption (1 photon of wavelength hυ) or two-photon absorption (2 photons of wavelength $h\upsilon_1$ and $h\upsilon_2$) via the virtual state (V). Fl is fluorescence, Ph is phosphorescence, and ISC is intersystem crossing.

The two-photon absorption cross section of a molecule is a quantitative measure of the probability of a two-photon absorption event occurring in a fluorophore.[10] The unit of the two-photon absorption cross section is the Göppert-Mayer or 'GM', where 1 GM = 10^{-50}

cm^4s/photon.[11] Physicist Maria Göppert–Mayer proposed the theoretical concept of multiphoton absorption in 1931 for the first time.[11] Other parameters used to measure the efficiency of the fluorophore are fluorescence quantum yields and two-photon action cross-sections. The fluorescence quantum yield is the number of photons emitted divided by the number of photons absorbed, measuring from 0 to 1. The action cross-section is the product of the fluorescence quantum yield and the two-photon absorption cross-section of the fluorophore, which indicates the brightness of the fluorophore. If the result of the action cross-section is high, the fluorophore can be useful in imaging. Usually, the squaraine dyes exhibit high fluorescence quantum yields and high two-photon absorption cross-sections, which is a good indication that the dyes can be useful for imaging applications. Two-photon fluorescence microscopy (2PFM) imaging is a powerful tool being used for studying biological function since it produces three-dimensional (3D) images with less damage to cells and lower fluorophore photobleaching (destruction of the excited state dye). The quadratic dependence of the intensity to the fluorophore absorption of a photon is what makes two-photon excitation so useful for fluorescence microscopy. The fluorescence is generated only within the minute focal volume, therefore all the fluorescence constitutes useful signals in fluorescence microscopy.[9] A molecule can act as a fluorophore when it has a conjugated system (every additional double bond shifts the spectra toward the infrared), and depends on the functional groups and the environment in which the fluorophore is found. The fluorescence wavelength of squaraine dyes normally falls in the near infrared region, providing deeper penetration through biological samples, such as thick tissue sections due to minimized absorption.[12] These squaraine dyes show an absorption band and a weakly stokes-shifted, mirror-image shaped fluorescence band in the near infrared region. Squaraine dyes that

could work for imaging cells and tissue for 2PFM imaging were synthesized and comprehensively characterized photophysically. The squaraine dyes were synthesized accordingly to function as a water-soluble fluorescent bioimaging dye that can serve as a probe for medical purposes. The prospective probes were used in cancer cells for imaging and analyzed to acquire data for early cancer detection and in the improvement of various therapies. Squaraine dyes were incubated with colorectal cancer (HCT-116) cells for evaluation. By binding to a molecule in one of the cell's organelle, the dye would be able to serve as a probe to mark carcinoma cells.

CHAPTER 2: EXPERIMENTAL SECTION

2.1 Materials

The following were purchased from ACROS, TCI or Sigma Aldrich: 2,3,3-trimethyl-3*H*-indole, 1,1,2-trimethyl-1*H*-benz[e]indole, iodoethane, iodododecane, iodooctadecane, 3,4-diethoxy-3-cyclobutene-1,2,-dione, 3,4-dihydroxy-3-cyclobutene-1,2-dione (Squaric acid), 9,9-diethyl-9*H*-fluorene, 1-methyl-1*H*-pyrrole-2-carboxaldehyde, triethyl ester phosphorous acid, 2,2-dioxide-1,2-oxathiolane (1,3-propanesultone), dichloromethane, absolute ethanol, toluene, n-butanol, ultra-pure water, hydrochloric acid, concentrated hydrochloric acid, sodium hydroxide pellets, pyridine, acetonitrile, diethyl ether, hexane, cyclohexane, dimethylsulfoxide (DMSO), poly-tetrahydrofuran (poly-THF), chloroform.

Cell Line. HCT-116 cell was purchased from America Type Culture Collection, ATCC, Manassas, VA, U.S.A. The incubation was done in RPMI-1640 medium purchased from Life Technologies (Grand Island, New York, U.S.A.), supplemented with 10% fetal bovine serum (FBS, Atlanta Biologicals, Lawrenceville, GA, U.S.A.) and 1% penicillin- streptomycin (Atlanta, GA, U.S.A.), and incubated at 37 ˚C in a 95% humidified atmosphere containing 5% CO_2. The cells were placed onto poly-D-lysine coated coverslips placed into 24-well glass plates 40,000 cells/well and incubated for 48hrs before incubating with the fluorescent probes.[13]

2.2 Measurements

Varian 300 or 500 MHz nuclear magnetic resonance (NMR) and a Bruker Avance III 400 MHz NMR spectrometers were used to measure ^{1}H and ^{13}C NMR spectra. The different solvents used were $CDCl_3$, CD_3OD, $(CD_3)_2SO$. The internal reference was tetramethysilane, TMS, at $\delta = 0.0$ ppm. In order to predict and analyze the ^{1}H and ^{13}C NMR spectra, CS ChemDraw Ultra version

11.0 and Mestrec Nova software were utilized. High-resolution mass spectrometry (HRMS) analysis was performed at the University of Florida's Department of Chemistry.

2.3 Synthesis

Details of the synthesis and characterization measurements of the intermediates and squaraine dyes **(10)**, **(8')**, **(9')** can be found in the following section, Results and Discussion.

Synthesis of Intermediates

The intermediate 2,7-bis(bromomethyl)-9,9-diethyl-9*H*-Fluorene **(7)** has been synthesized in the past in the laboratory.[14]

Synthesis of 3-ethyl-1,1,2-trimethyl-1H-benz[e]indolium iodide (2)

1,1,2-trimethyl-1*H*-benz[e]indole **(1)** was used for the synthesis of **(2)**. A mixture of **(1)** (2.0 g, 9.6 mmol) and CH_2CH_3I (1.5 g, 9.6 mmol) was mixed in a microwave tube in acetonitrile (3 mL). The mixture was degassed by nitrogen or argon for 20 min, and then microwaved at 150 ˚C, 150 psi, 120 W for 20 min. The solvent was evaporated and the resulting solid was filtered and washed with ethyl ether to afford 3.6 g of yellow crystals (82% yield). Melting point: 219 ˚C. ^{1}H NMR (300 MHz, ($CDCl_3$) δ: 8.15 – 8.01 (m, 3H), 7.82 (m, 1H), 7.70 (m, 2H), 4.88 (q, *J* = 7.4 Hz, 2H), 3.23 (d, *J* = 2.0 Hz, 3H), 1.87 (d, *J* = 1.7 Hz, 6H), 1.70 – 1.63 (m, 3H).

Synthesis of (Z)-3-ethoxy-4-((3-ethyl-1,1-dimethyl-1H-benzo[e]indol-2(3H)-ylidene)methyl)cyclobut-3-ene-1,2-dione (4)

A 10% sodium hydroxide solution was prepared, mixed with hexane and compound **(2)** (1 g, 2.7 mmol). The mixture was agitated until all the salt had reacted with base. The deprotonated product was collected by extracting with the organic layer in a separatory funnel. The solvent

was evaporated and the product was immediately mixed with compound **(3)** (0.47 g, 2.7 mmol). This mixture was refluxed in absolute ethanol (10 mL) and triethylamine (1 mL) for 10-20 min and follow by TLC. Upon cooling, the precipitates were collected by filtration and carefully wash with hexane, and dried in vacuum, affording 0.971 g of a yellow solid (98% yield). Recrystallization from ethanol gave an analytical pure sample. Melting point 163 ℃. ^{1}H NMR (300 MHz, $(CD_3)_2SO$) δ: 8.09 (d, *J* = 8.7 Hz, 1H), 7.85 (m, 2H), 7.52 (m, 1H), 7.36 (m, 1H), 7.23 (m, 1H), 5.44 (d, *J* = 2.8 Hz, 1H), 4.92 (m, 2H), 3.99 (m, 2H), 1.89 (s, *J* = 2.5 Hz, 6H), 1.55 (m, 3H), 1.37 (m, 3H).

Synthesis of (Z)-3-((3-ethyl-1,1-dimethyl-1H-benzo[e]indol-2(3H)-ylidene)methyl)-4-hydroxycyclobut-3-ene-1,2-dione (5)

Compound **(4)** (0.5 g, 1.4 mmol) was dissolved in boiling absolute ethanol and mixed with 40% sodium hydroxide solution (~15 drops), which is added dropwise until all the material has reacted. The reaction was followed by TLC. After all the starting material has reacted, the reaction is cool down and the pH was brought down using diluted hydrochloric acid to an acidic pH of about 3. The solvent is evaporated and the resulting solid is dissolved in dichloromethane. Using gravity filtration, the product is separated from the salt. The dichloromethane is evaporated and brown flakes are collected as the final product (0.44 g, 94%). ^{1}H NMR (400 MHz, CD_3CN) δ: 8.15 (d, *J* = 8.5 Hz, 1H), 7.91 (t, *J* = 8.2 Hz, 2H), 7.59 (t, *J* = 7.7 Hz, 1H), 7.43 (t, *J* = 7.6 Hz, 1H), 7.27 (s, 4H), 5.74 (s, 1H), 4.13 (d, *J* = 7.2 Hz, 2H), 3.55 – 3.34 (m, 5H), 1.96 (d, *J* = 3.1 Hz, 6H), 1.45 (t, *J* = 7.2 Hz, 3H).

Synthesis of 2,2'-((1E,1'E)-(9,9-diethyl-9H-fluorene-2,7-diyl)bis(ethene-2,1-diyl))bis(1-methyl-1H-pyrrole) (9)

A mixture of 2,7-bis(bromomethyl)-9,9-diethyl-9*H*-Fluorene **(7)** (1.5 g, 3.7 mmol) and triethyl phosphite (5 mL) was reflux for 2hrs under N_2. Excess Triethyl phosphite was distilled under reduced pressure. The residue was dried under vacuum and used directly for the Horner-Emmons reaction. The intermediate was dissolved in dry DMF (5 mL), followed by slow addition of NaH (1.76 g, 73.3 mmol). The mixture was reacted under N_2 atmosphere at room temperature for 1hr, follow by addition of 1-methyl-1H-pyrrole-2-carbaldehyde (0.8 g, 7.3 mmol). The mixture was then stirred overnight at room temperature. Water was added and the precipitate was collected by filtration, carefully washed with water and dried. The crude product was purified by column chromatography with hexane/dichloromethane 2:1 as eluent. A yellow powder was obtained (1.09 g, 69%). ^{1}H NMR (500 MHz, $(CD_3)_2CO$) δ: 7.63 (m, 2H), 7.44 (m, 2H), 7.37 (t, *J* = 1.9 Hz, 2H), 7.07 – 6.89 (m, 4H), 6.64 (m, 2H), 6.50 (m, 2H), 6.16 (m, 2H), 3.73 (d, *J* = 1.4 Hz, 6H), 2.07 (q, *J* = 7.3 Hz, 4H), 0.46 – 0.30 (m, 6H).

Synthesis of (4E,4'E)-2,2'-(5,5'-(1E,1'E)-2,2'-(9,9-diethyl-9H-fluorene-2,7-diyl)bis(ethene-2,1-diyl)bis(1-methyl-1H-pyrrole-5,2-diyl))bis(4-((3-ethyl-1,1-dimethyl-1H-benzo[e]indolium-2-yl)methylene)-3-oxocyclobut-1-enolate) (10)

A mixture of compound **(5)** (0.25 g, 0.75 mmol) and **(9)** (164 mg, 0.38 mmol) were refluxed under N_2 with a Dean-Stark apparatus overnight in 1:2 Toluene/Butanol. The solvent was evaporated and the product was purified using preparative TLC with dichloromethane/methanol 200:1 as eluent giving 80 mg of dark blue-bright fuchsia powder **(10)**. (20% yield) decomposed at 210-220ºC. ^{1}H NMR (400 MHz, $CDCl_3$) δ: 8.23-8.21 (d, *J* = 8.0 Hz, 1H), 7.96-7.94 (d, *J* = 8.0

Hz, 2H), 7.73-7.70 (t, *J* = 6.0 Hz, 2H), 7.66-7.62 (t, *J* = 8.0 Hz, 1H), 7.55-7.48 (m, 3H), 7.40-7.38 (d, *J* = 8.0 Hz, 1H), 7.30-7.26 (d, *J* = 16.0 Hz, 1H), 7.16-7.12 (d, *J* = 16.0 Hz, 1H), 6.88-6.87 (d, *J* = 4.0 Hz, 1H), 6.18 (s, 1H), 4.38 (s, 3H), 4.35-4.30 (m, 2H), 2.16- 2.09 (m, 2H), 2.11 (s, 6H), 1.54-1.50 (t, *J* = 8.0 Hz, 3H), 0.42-0.38 (t, *J* = 8.0 Hz, 3H). ^{13}C NMR (101 MHz, $CDCl_3$) δ: 182.42, 174.38, 163.75, 151.08, 143.22, 143.04, 141.67, 138.40, 136.07, 135.91, 135.20, 132.86, 131.90, 130.13, 129.79, 128.49, 128.40, 127.70, 126.23, 125.18, 125.02, 122.70, 120.94, 120.72, 120.24, 114.89, 112.12, 110.17, 88.46, 77.21, 56.20, 52.19, 39.36, 33.99, 32.90, 29.69, 26.39, 26.30, 23.43, 12.72, 8.59. HRMS (ESI-TOF) theoretical *m*/*z* = 1062.5090 (M^+), found *m*/*z* = 1062.5054 (M^+).

Synthesis of 3-(2,3,3-trimethyl-3H-indol-1-ium-1-yl)propane-1-sulfonate (3')

2,3,3-trimethyl-3*H*-indole **(1')** (1 g, 6.3 mmol) was heated under reflux with an equimolar amount of 1,3-propanesultone **(2')** (0.78 g, 6.4 mmol) in toluene (15 mL) overnight, with constant stirring. Upon cooling, the product was separated by filtration, washed with dichloromethane and dried under vacuum giving a red-pink powder that was used without further purification.[15] (1.7 g, 94%). ^{1}H NMR (400 MHz, DMSO-d6) δ: 8.10 – 8.00 (m, 1H), 7.86 – 7.77 (m, 1H), 7.68 – 7.56 (m, 2H), 4.74 – 4.59 (m, 2H), 2.84 (s, 3H), 2.63 (t, *J* = 6.5 Hz, 2H), 2.24 – 2.10 (m, 2H), 1.54 (s, 6H).

Synthesis of 1-dodecyl-2,3,3-trimethyl-3H-indol-1-ium iodide (6')

2,3,3-trimethyl-3*H*-indole **(1')** was used for the synthesis of **(6')**. A mixture of **(1')** (1.0 g, 6.3 mmol) and $C_{12}H_{25}I$ (1.9 g, 6.4 mmol) was mixed in a microwave tube in acetonitrile (3 mL). The mixture was degassed by nitrogen or argon for 20 min, and then microwaved at 150 ˚C, 150 psi,

120 W for 60 min. The solvent was evaporated and the resulting wax was washed with ethyl ether several times to afford 0.5231 g of brown-orange wax (28% yield). ^{1}H NMR (400 MHz, Chloroform-d) δ: 7.60 – 7.57 (m, 2H), 7.53 – 7.49 (m, 2H), 4.72 – 4.66 (m, 2H), 3.12 (s, 3H), 1.98 – 1.88 (m, 2H), 1.67 (s, 6H), 1.47 (m, 2H), 1.40 – 1.34 (m, 2H), 1.31 – 1.23 (m, 14H), 0.91 – 0.85 (m, 3H).

Synthesis of 1-octadecyl-2,3,3-trimethyl-3H-indol-1-ium iodide (7')

2,3,3-trimethyl-3*H*-indole **(1')** was used for the synthesis of **(7')**. A mixture of **(1')** (1.0 g, 6.3 mmol) and $C_{18}H_{37}I$ (2.4 g, 6.3 mmol) was mixed in a microwave tube in acetonitrile (3 mL). The mixture was degassed by nitrogen or argon for 20 min, and then microwaved at 150 ˚C, 150 psi, 120 W for 60 min. The solvent was evaporated and the resulting solid was filtered and washed with ethyl ether to afford 1.25 g of a yellow powder (37% yield). ^{1}H NMR (500 MHz, Chloroform-d) δ: 7.67 – 7.63 (m, 1H), 7.60 – 7.57 (m, 3H), 4.72 – 4.65 (m, 2H), 3.13 (s, 3H), 1.98 – 1.90 (m, 2H), 1.67 (s, 6H), 1.51 – 1.42 (m, 2H), 1.39 – 1.34 (m, 2H), 1.29 – 1.23 (m, 26H), 0.92 – 0.84 (m, 3H).

Synthesis of (E)-2-((E)-(3,3-dimethyl-1-(3-sulfopropyl)indolin-2-ylidene)methyl)-4-((1-dodecyl-3,3-dimethyl-3H-indol-1-ium-2-yl)methylene)-3-oxocyclobut-1-enolate (8')

A mixture of compound **(3')** (0.69 g, 2.45 mmol), **(6')** (1.11 g, 2.44 mmol) and Squaric acid (0.29 g, 2.54 mmol) were refluxed under N_2 with a Dean-Stark apparatus overnight in 1:1:0.1 Toluene/Butanol/pyridine. The solvent was evaporated and the product was purified using preparative thin layer chromatography (TLC) with dichloromethane/methanol 20:1 as eluent giving 78.2 mg dark blue flakes **(8')**. (4% yield). ^{1}H NMR (400 MHz, Chloroform-d) δ: 7.27 (s,

5H), 7.09 – 6.98 (m, 3H), 6.90 (d, *J* = 8.0 Hz, 2H), 6.35 (s, 2H), 5.84 (s, 2H), 4.40 (s, 4H), 3.89 (s, 4H), 3.22 (s, 4H), 2.64 (s, 2H), 2.28 (s, 5H), 1.72 (t, *J* = 5.0 Hz, 1H), 1.37 (d, *J* = 7.0 Hz, 2H), 1.33 – 1.19 (m, 26H), 0.91 – 0.83 (m, 6H). ^{13}C NMR (126 MHz, Chloroform-d) δ: 175.35 , 170.84 , 143.16 – 140.87 (m), 128.09 , 127.62 , 123.94 , 122.34 , 122.00 , 110.02 (d, *J* = 7.7 Hz), 109.33 , 86.01 , 49.18 (d, *J* = 6.0 Hz), 47.87 , 43.75 , 42.47 , 31.90 , 30.48 – 28.95 (m), 27.37 – 26.46 (m), 22.68 , 22.52 , 14.12. HRMS (ESI-TOF) theoretical *m*/*z* = 686.3748 (M^+), found *m*/*z* = 687.3836 ($[M + H]^+$).

Synthesis of (E)-2-((E)-(3,3-dimethyl-1-(3-sulfopropyl)indolin-2-ylidene)methyl)-4-((3,3-dimethyl-1-octadecyl-3H-indol-1-ium-2-yl)methylene)-3-oxocyclobut-1-enolate (9')

A mixture of compound **(3')** (0.26 g, 0.92 mmol), **(7')** (0.50 g, 0.93 mmol) and Squaric acid (0.105 g, 0.92 mmol) were refluxed under N_2 with a Dean-Stark apparatus overnight in 1:1:0.1 Toluene/Butanol/pyridine. The solvent was evaporated and the product was purified using preparative TLC with dichloromethane/methanol 15:1 as eluent giving 56 mg dark blue powder **(9')**. (8% yield). ^{1}H NMR (500 MHz, Chloroform-d) δ: 7.19 (dt, *J* = 22.2, 6.0 Hz, 4H), 7.10 – 6.88 (m, 3H), 6.86 (d, *J* = 7.8 Hz, 1H), 6.24 (s, 1H), 5.81 (s, 1H), 4.36 (s, 2H), 3.85 (s, 2H), 3.22 (s, 2H), 3.02 (s, 3H), 2.29 – 2.20 (m, 2H), 1.61 (d, *J* = 6.4 Hz, 12H), 1.48 – 0.97 (m, 32H), 0.87 (t, *J* = 6.7 Hz, 3H). ^{13}C NMR (500 MHz, Chloroform-d) δ: 170.66 , 170.12 , 142.19 , 142.06 , 141.90 , 128.07 , 127.57 , 123.84 , 123.75 , 122.31 , 121.94 , 110.02 , 109.22 , 87.22 , 86.06 , 49.14 , 47.83 , 43.69 , 42.47 , 31.92 , 29.69 (d, *J* = 5.7 Hz), 29.62 , 29.57 , 29.51 , 29.35 (d, *J* = 2.5 Hz), 27.11 – 26.70 (m), 22.69 , 14.12. HRMS (ESI-TOF) theoretical *m*/*z* = 771.4765 (M^+), found *m*/*z* = 771.4768 (M^+).

2.4 Linear and Non-linear Photophysical Properties

An Agilent (Model 8453) diode-array spectrometer was utilized for Ultraviolet–visible (UV-vis) absorption spectroscopy. Concentrations of ≈ 1×10^{-6} M of the squaraine dyes (**10)**, **(8')**, **(9')** were prepared in chloroform (for dye SQ **(10)**), and DMSO (for dye SQ (**8')**, SQ **(9')**) at room temperature in 1 cm quartz cuvettes. Fluorescence emission measurements were obtained using a PTI International, Model MD-5020 fluorimeter. The quantum yields were calculated using a comparative method against Rhodamine 6G. Excitation anisotropy spectra were measured with a PTI Quantamaster spectrofluorimeter equipped with a photomultiplier tube (PMT) in high viscosity solvent (poly-THF). The two-photon absorption (2PA) cross section of the squaraine dyes were determined using femtosecond Ti:sapphire laser excitation sources. From 700 to 1000 nm data is collected with a silicon detector and from 1000 to 1400nm data is collected with a germanium detector.

2.5 Cytotoxicity (MTS) Assay Procedure

To evaluate the cytotoxicity of the squaraine dyes **(8')**and (**9')**, a cell viability test was performed using 5×10^3 cells/well of HCT-116 cells in 96-well plates were incubated in 100 μL of RPMI-1640, supplemented 10% Fetal Bovine Serum (FBS) and 1% penicillin-streptomycin for 48 hrs. Then the cells were incubated with several concentrations of dye **(8')** (1, 5, 10, 25, 50μM), respectively, and (**9')** (1.3, 3.1, 6.3, 12.5, 25, 50, 100 μM), respectively, for an additional 22 hrs. Next, 20 μL of CellTiter 96 AQueous One Solution reagent was added into each well, followed by further incubation for 2 hrs at 37 ˚C. The relative viability of the HCT-116 cells incubated with probes (**8')** and **(9')** to unaltered cells was determined by subtracting the absorbance of the cell-free medium blank (volume at 490 nm) by the absorbance of the MTS-formazan on a

microplate reader (Spectra Max M5, Molecular Devices, Sunnyvale, CA, U.S.A.) at 490 nm. Three individual experiments were prepared and averaged.[13] See **Figure 5** to follow a scheme of how the procedure was completed.

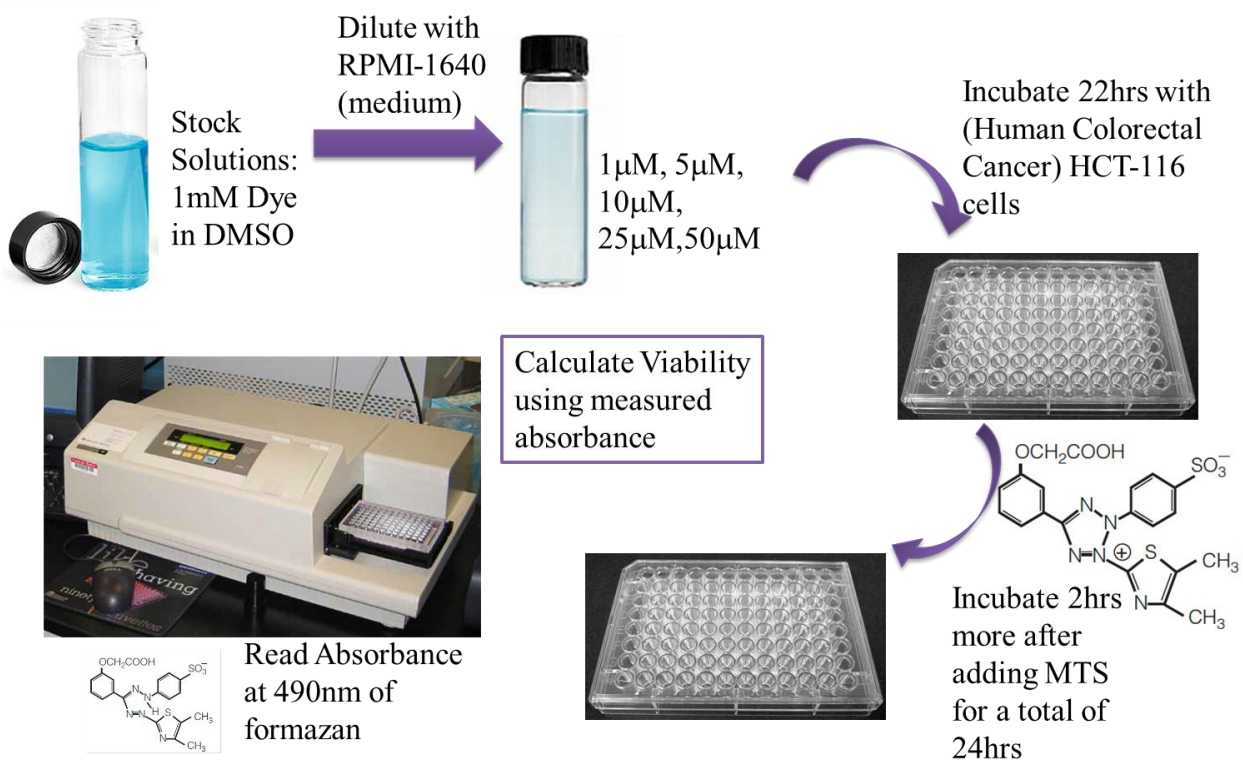

Figure 5. Cytoxicity (MTS) Assay procedure.

2.6 Cell Culture and Incubation

HCT-116 cells were placed onto poly-D-lysine coated glass coverslips in 24-well plates (40,000 cells per well), and the cells were incubated for 48 hrs before incubating with the squaraine dye (**8'**) and (**9'**). A 1mM stock solution of SQ (**8'**) and SQ (**9'**) was prepared in DMSO. The solution was diluted to 15 μM with RPMI-1640 and lysoTracker Red, and then incubated for a period of an hour. Following incubation, the cells were washed with PBS (x 3) and fixed using 3.7% formaldehyde solution for 10 min at 37 °C. Then freshly prepared $NaBH_4$ (1 mg/mL, prepared

by adding few drops of 6 N NaOH solution in $NaBH_4$ solution) solution in PBS (pH = 8.0) was added to each well (0.5 mL/well) for 10 min (x 2) (in order to decrease autofluorescence). Afterwards the plates were washed with PBS (x 2) and water. Lastly, the coverslips were mounted using Prolong Gold mounting media (Life Technologies) for microscopy.[13] See **Figure 6** for an scheme of how the procedure is completed.

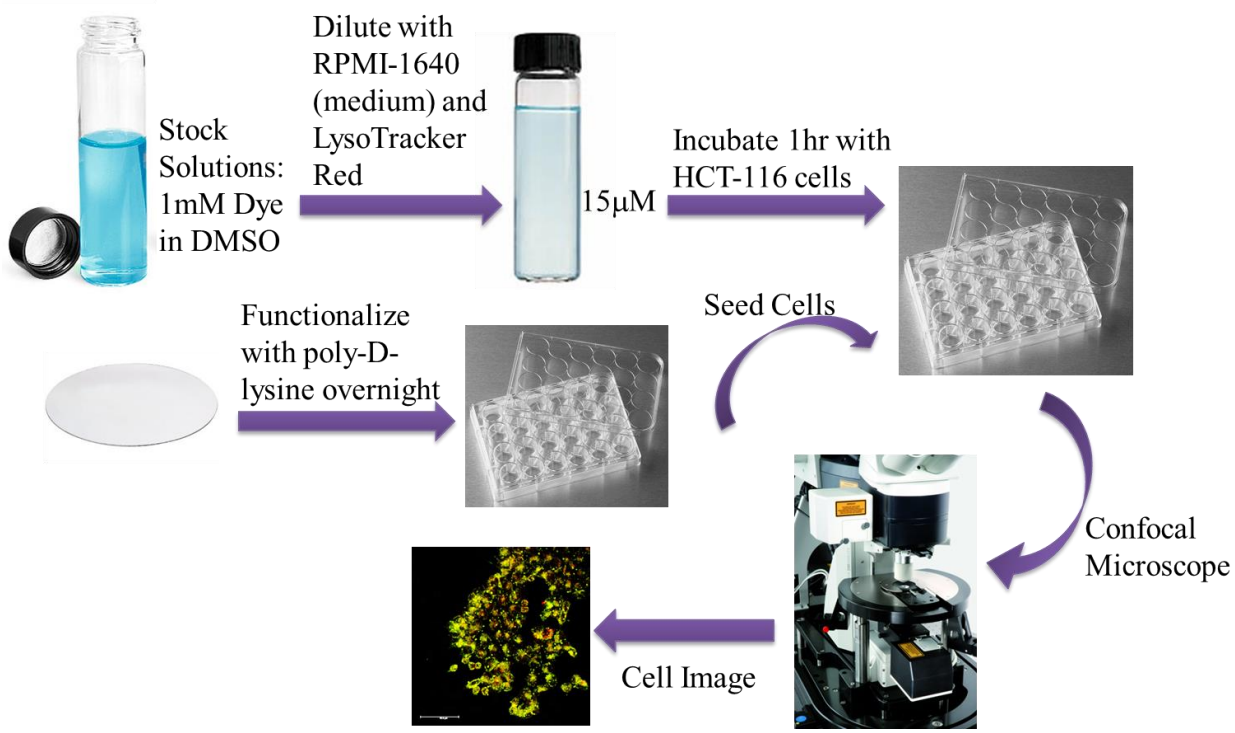

Figure 6. Cell incubation and imaging procedure.

2.7 One-Photon Fluorescence Microscopy (1PFM) Imaging

All the images were recorded on a Leica TCS SP5 II laser-scanning confocal microscope system. A water immersion 63x objective (HCX Pl APO CS 63.0×1.20 WATER UV) was used. For one-photon imaging of the squaraine dyes (**8'**) and (**9'**), cells were excited at 633 nm. Fluorescence was collected in a range from 650 to 680 nm. For one-photon imaging of the lysoTracker Red for

colocalization, the cells were excited at 561 nm. Fluorescence was collected in a range from 580 to 630 nm. The confocal pinhole was applied for better image quality.

2.8 Two-Photon Fluorescence Microscopy (2PFM) Imaging

For two-photon imaging, the Leica TCS SP5 II microscope system, coupled to a tunable Coherent Chameleon Vision S (80 MHz, modelocked, 75 fs pulse width, tuned to 700 nm). The cells were excited at 800nm. An NDD detector (617/73) was used to collect two-photon fluorescence.

CHAPTER 3: RESULTS & DISCUSSION

3.1 Synthesis

Figure 7 shows the synthetic steps for the preparation of (4E,4'E)-2,2'-(5,5'-(1E,1'E)-2,2'-(9,9-diethyl-9H-fluorene-2,7-diyl)bis(ethene-2,1-diyl)bis(1-methyl-1H-pyrrole-5,2-diyl))bis(4-((3-ethyl-1,1-dimethyl-1H-benzo[e]indolium-2-yl)methylene)-3-oxocyclobut-1-enolate), (**10)**. Two different intermediates were prepared via two routes to combine and obtain the final target dye.

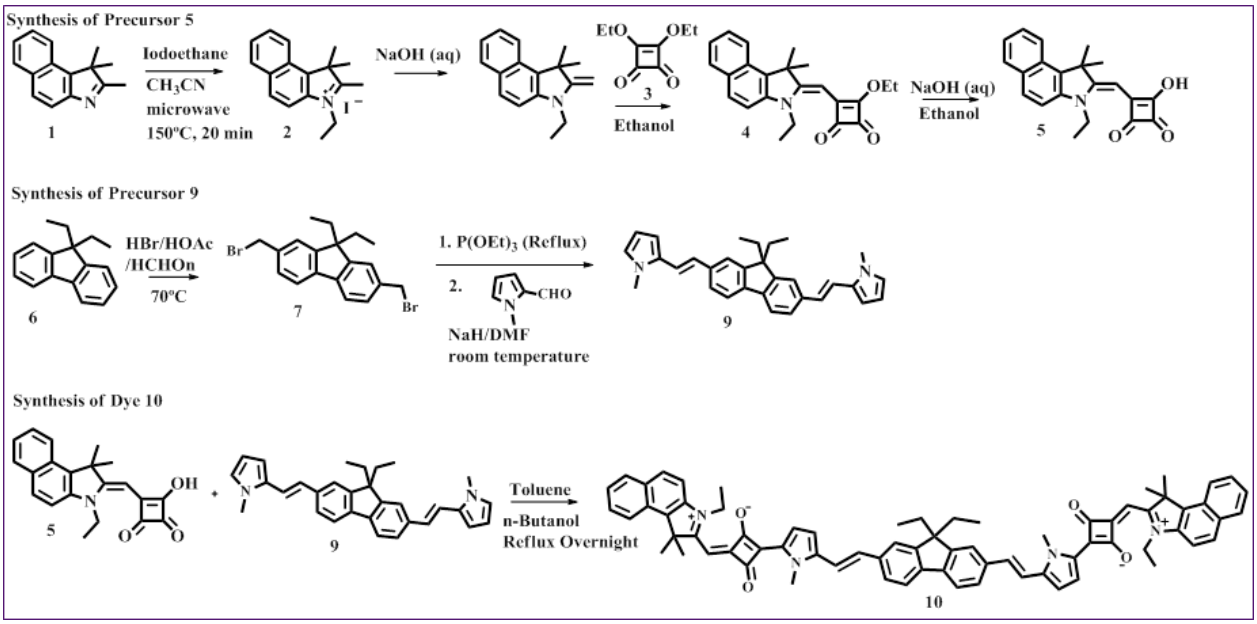

Figure 7. Synthesis of (4E,4'E)-2,2'-(5,5'-(1E,1'E)-2,2'-(9,9-diethyl-9H-fluorene-2,7-diyl)bis(ethene-2,1-diyl)bis(1-methyl-1H-pyrrole-5,2-diyl))bis(4-((3-ethyl-1,1-dimethyl-1H-benzo[e]indolium-2-yl)methylene)-3-oxocyclobut-1-enolate) SQ **(10)**.

Intermediate (**2)** was synthesized by the alkylation of the nitrogen atom on the benzoindole compound (**1)** using iodoethane. The two starting materials were mixed in the solvent acetonitrile, which can be evaporated at the end of the reaction to precipitate the crude product.

The reaction was followed by TLC. The reaction did not react completely; leaving starting materials unreacted, mixed in with the product. The unreacted starting material was removed when the crude product was filtered and washed with ethyl ether. The product was characterized using proton NMR. Two new peaks appeared in the aliphatic region, a triplet for the methyl group and quartet for the methylene group. In addition, the starting material **(1)** was not completely pure. It came with a small percentage of its isomer, making it a mixture product. This isomer reflects in the NMR of all of the products, and it was difficult to isolate.

Intermediate **(4)** was prepared from a methylene base intermediate product that resulted from the deprotonation of the benzoindolium salt **(2)** at the methyl located on the second carbon produced in the previous step and a substitution reaction with diethyl squarate immediately. (This was a one pot reaction.) The deprotonation was done with aqueous sodium hydroxide and as the product formed, it dissolved in hexane, which was mixed together in the solution. This product was very unstable, it can be oxidized within minutes after its preparation, hence the reason why the diethyl squarate was added to react with the intermediate directly. Therefore, this intermediate must be prepared carefully, to obtain a higher percent yield. In addition to following the reaction by TLC, the product was also characterized by proton NMR. One of the main changes noted in the spectrum was the appearance of a singlet for the proton in the alkene, and the disappearance of the singlet for three protons corresponding to the methyl group on the same carbon. Also, a new quartet for the methylene next to the oxygen and a triplet for the methyl group also confirm the product was obtained.

The precursor **(5)**, which was one step before the condensation reaction to make the dye, should only be prepared if it is going to be used promptly. This product was also very unstable; it

decomposes rapidly when left unused. The hydrolize reaction of intermediate **(4)** was very fast and had a high percent yield. Therefore it can be prepared last, after the preparation of precursor **(9)** to make the final target dye and obtain higher yields. Precursor **(5)** was characterized using proton NMR. The main peak to look for are the appearance of a broad singlet, in either the aliphatic region or far downfield past the aromatic region, corresponding to the proton of the hydroxyl group, in addition to the disappearance of the quartet and triplet, corresponding to the methylene and methyl groups in the ethoxy that is removed.

The preparation of precursor **(9)** was also completed using a one pot reaction. The reaction had excess reagent that could be isolated from the crude product. This reaction gave two different alkenes isomer as the final product, but the *E*-alkene is highly favored. The product had different R_f values compared, to starting material, making the separation straightforward. Once this precursor was prepared and precursor **(5)** was obtained, the two starting materials were mixed in toluene and butanol to reflux, in order to make the final dye from a condensation reaction.

Isolating the desired dye **(10)** from the crude product of the condensation reaction is more work. The reaction produced many of by-products and unreacted starting material. A by-product that this reaction yielded was the mono-substituted molecule. In addition, these compounds can decompose or oxidize if not carefully prepared. The product was characterized using proton and carbon NMR and high resolution mass spectrometry. The final target was very hydrophobic. Therefore, its linear and non-linear properties were not measured in polar solvents. Since the dye was hydrophobic, it exhibited poor solubility in water, thus had to be encapsulated in micelles to incubate the dyes with the cells. The dye was then inserted into Pluronic micelles, but the

fluorescence of the dye was quenched. One reason the fluorescence of the dye could have been quenched once inserted into Pluronic micelles, was because the dye aggregated.

A synthesis of an amphiphilic structure was proposed and accomplished, in order to resolve the issue of fluorescence quenching when inserting a hydrophobic dye in micelles. An amphiphilic dye can act as a micelle itself, but the fluorescence of the dye would not be quenched since if does not aggregate. The dye can be dissolved in polar solvents such as DMSO and water, which gives the advantage of incubating the dye with the cells with greater ease.

Figure 8 shows the synthetic route used to obtain both of the amphiphilic squaraine dyes prepared (E)-2-((E)-(3,3-dimethyl-1-(3-sulfopropyl)indolin-2-ylidene)methyl)-4-((1-dodecyl-3,3-dimethyl-3H-indol-1-ium-2-yl)methylene)-3-oxocyclobut-1-enolate **(8')** and (E)-2-((E)-(3,3-dimethyl-1-(3-sulfopropyl)indolin-2-ylidene)methyl)-4-((3,3-dimethyl-1-octadecyl-3H-indol-1-ium-2-yl)methylene)-3-oxocyclobut-1-enolate **(9')**.

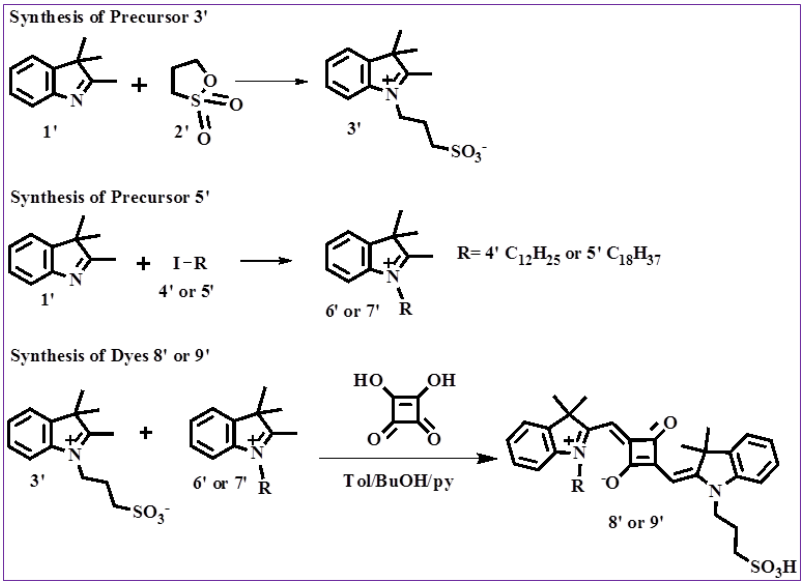

Figure 8. Synthesis of squaraine dyes (E)-2-((E)-(3,3-dimethyl-1-(3-sulfopropyl)indolin-2-ylidene)methyl)-4-((1-dodecyl-3,3-dimethyl-3H-indol-1-ium-2-yl)methylene)-3-oxocyclobut-1-enolate SQ **(8')** and (E)-2-((E)-(3,3-dimethyl-1-(3-sulfopropyl)indolin-2-ylidene)methyl)-4-((3,3-dimethyl-1-octadecyl-3H-indol-1-ium-2-yl)methylene)-3-oxocyclobut-1-enolate SQ **(9')**.

The synthesis of precursor **(3')** was completed directly from the literature, with one minor change. After the nitrogen in the indole compound attacked the carbon adjacent to the oxygen, to open the five member ring, the desired product was obtained. The analytical pure product was obtained after washing the solid with dichloromethane, instead of washing with hexane, as was suggested in the literature. The product was characterized using proton NMR. In the spectrum, the appearance of three new peaks was noted for the three methylene group. The CH_2 group closer to the nitrogen would further downfield above 4ppm than the others in the aliphatic region, which are usually found next to the methyl group peaks.

The synthesis of precursor **(6')** was completed by the alkylation of indole with dodecyl iodide, and it was followed by TLC. This reaction was also done in the microwave at 150 °C, 150 psi, but instead of 20 min like the benzoindole alkylation, it was reacted for 60 min. This reaction had many by-products and yielded a sticky product. To obtain a pure product, the sticky compound was placed in ethyl ether many times in a sonicator, to wash out the impurities and any starting material left unreacted. The product was then characterized using proton NMR. The same synthesis procedure was followed for the precursor **(7')**, but obtained a purified solid. Once these salts were synthesized they can be used for the synthesis the final target squaraine dyes.

The dyes SQ **(8')** and SQ **(9')** are very stable dyes. There are not sensitive to air and do not decompose when placed in silica. Both dyes were prepared using the same procedure of mixing precursor **(3')**, squaric acid and the respective salt **(6')** or **(7')**. These synthesis yielded many by-products, including di-substitution of the indolium salts, or di-substitutions of the indolium sulfhydryl propyl salt. For this reason, the best way to purify the product was using preparative TLC to obtain the highest yield possible. The two reactions, however, produced a relatively low

percent yield, since there were many by-products, and starting material that did not react. The two squaraine dyes were characterized using proton and carbon NMR and high resolution mass spectrometry. Both of these products achieved emission in the near-infrared region and were able to be dissolved in DMSO and aqueous media to incubate the dyes with cancer cells. These results are further explained in the linear and non-linear photophysical properties and cell viability study section below.

3.2 Linear and Non-linear Photophysical Properties

The linear and non-linear photophysical properties of squaraine dyes **(10)**, **(8')**, **(9')** are shown in **Table 1**. The UV-vis absorption, emission, fluorescence quantum yield (which is a measure of emission efficiency, measuring the number of photons emitted per number of photons absorbed), anisotropy (which characterizes polarizability) and two-photon absorption of SQ **(10)** were carefully characterized in chloroform (except the anisotropy, which uses poly-THF) (**Figure 10**). Rhodamine 6G was used as the reference. All emission spectra were corrected by the spectral sensitivity of the PMT. In chloroform, the absorption λ_{max} was 719 nm and emission λ_{max} was 738 nm. The stoke shift for this dye was relatively small, up to 19 nm, which is a common attribute for this class of compounds. The emission spectra was used for determination of the relative fluorescence quantum yield, $\boldsymbol{\Phi_{FL}}$, using the formula shown in **Figure 9a**.[13] The fluorescence quantum yield ($\boldsymbol{\Phi_{FL}}$) was found to be 0.38 ± 0.01. The $\boldsymbol{\Phi_{FL}}$ of the dye in water-soluble micelles decreased significantly. Commonly, the fluorescence of the dyes decrease when placed in polar solvents; also in micelles, the dyes aggregate which increases the fluorescence quenching process.[13] The excitation anisotropy spectrum was recorded using a previous reported method, calculated with the equation shown in **Figure 9b**. "Excitation anisotropy is different for different

electronic transitions of a molecule, and is based on the angle between the absorption and emission dipole moments."[13] The values of anisotropy theoretically ranges from -0.2 to +0.4, due to the angles between transition dipole moments.[13] Therefore, the spectrum of excitation anisotropy can be used to estimate electronic transitions of the dye. This gives the advantage of estimating one-photon forbidden transitions and two-photon allowed transitions, since the selection rules for one-photon and two-photon absorption are different.[13] Squaraine dye **(10)** solution was prepared in poly-THF, a highly viscous solvent that restricts the rotation of the molecules, avoiding molecular reorientation. Usually, a plateau is associated with one-photon allowed transitions ($S_0 \rightarrow S_1$) and two-photon forbidden transitions. The changes observed in the spectra creating minima and maxima values suggest different electronic transitions ($S_0 \rightarrow S_n$) that are potentially two-photon allowed transitions.[13] In the excitation anisotropy spectrum of dye **(10)**, the transitions are more complex to identify. However, an estimate of where a 2PA allowed transition can still be made by observing the changes and minimum value that occurs around 500 nm in the spectrum. This analysis of the excitation anisotropy spectrum correlated well with the observed wavelength-dependent 2PA cross-sections as shown in **Figure 10**. The recorded cross-section was 2600 GM at 940 nm, which is an interesting parameter that is looked for, as explained before. The dyes should have high 2PA cross-sections to serve as a probe. The photophysical properties studied for dyes SQ **(8')** and SQ **(9')** were carefully characterized in DMSO. Rhodamine 6G was used as well for the reference. Both dyes exhibited an absorption λ_{max} of 645 nm and an emission λ_{max} of 653 nm. The fluorescence quantum yield ($\mathbf{\Phi_{FL}}$) measured as mentioned previously, was found for dye SQ **(8')** to equal to 0.36 ± 0.01. Since, both dyes SQ **(8')** and SQ **(9')** have the same conjugated system and exhibit the same linear properties, the

non-linear properties measurements for dye **(9')** were not measured and assumed to be the same or very similar to the properties of dye **(8')**. The investigated 2PA cross-section maximum for dye (8') was above 1700 GM at 740nm and this value did not exactly coincide with the anisotropy minimum, although it was close, indicating possible higher $S_0 \rightarrow S_n$ electronic transitions.[13] **Figures 11** and **12** shows the photophysical properties for both of these squaraine dyes.

Table 1. Summary of the normalized UV-visible absorbance and fluorescence emission spectra, fluorescence quantum yield, stokes shift and cross-sections values of dyes SQ **(10)**, SQ **(8')**, SQ **(9')**.

Compound	**Solvent**	**Absorption λ_{max} (nm)**	**Emission λ_{max} (nm)**	**Stokes Shift**	**Φ_{FL}**	**2PA cross-sections (GM)**
10	Chloroform	719	738	19	0.38 ± 0.04	2600
8'	DMSO	645	653	8	0.36 ± 0.01	1700
9'	DMSO	645	653	8	----------	--------

a. $$\boldsymbol{\Phi_{FL}} = \boldsymbol{\Phi_R} \frac{I}{I_R}\frac{OD_R}{OD}\frac{n^2}{n_R^2}\frac{RP_R}{RP}$$

Φ = Quantum yield
I = Integrated Data
OD = Optical Density
n = Refractive Index (of solvent)
RP = Relative Power (of source beam)
Subscript R = Reference

b. $$\boldsymbol{r} = \frac{l_{VV} - GI_{VH}}{l_{VV} + 2GI_{VH}}, \left(G = \frac{I_{HV}}{I_{HH}}\right)$$

r = anisotropy
G = ratio of sensitivities for polarized light
V = vertically polarized light
H = horizontally polarized light
I = fluorescence intensity

Figure 9. a. Fluorescence Quantum Yield Formula.[13] b. Anisotropy Formula.[13]

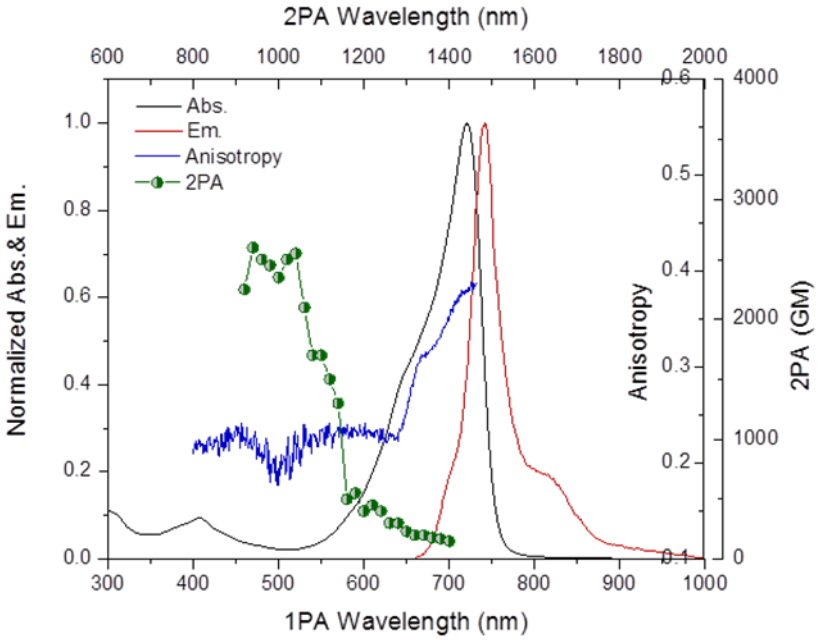

Figure 10. Fluorescence quantum yield was 0.38 ± 0.04 measured in chloroform. Absorption and emission spectra of squaraine dye **(10)** in chloroform. λ_{max} = 719 nm for the absorption and λ_{max} = 738 nm for emission. Anisotropy in poly-THF. With a 2PA λmax = 940nm and δ = 2600 GM.

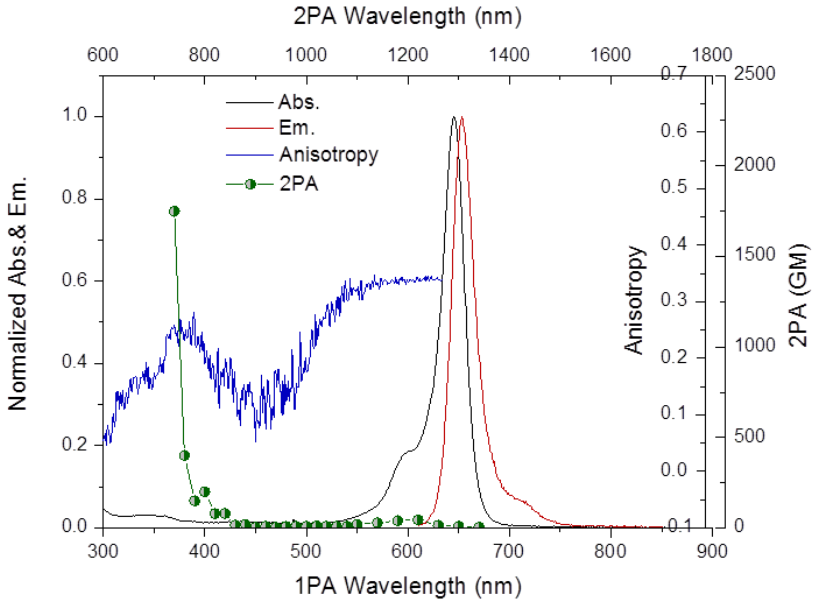

Figure 11. Fuorescence quantum yield was 0.36 ± 0.04 measured in DMSO. Absorption and emission spectra of squaraine dye **(8')** in DMSO. λ_{max} = 645 nm for absorption and λ_{max} = 653 nm for emission. Anisotropy in poly-THF. With a 2PA λmax = 740nm and δ = 1700 GM.

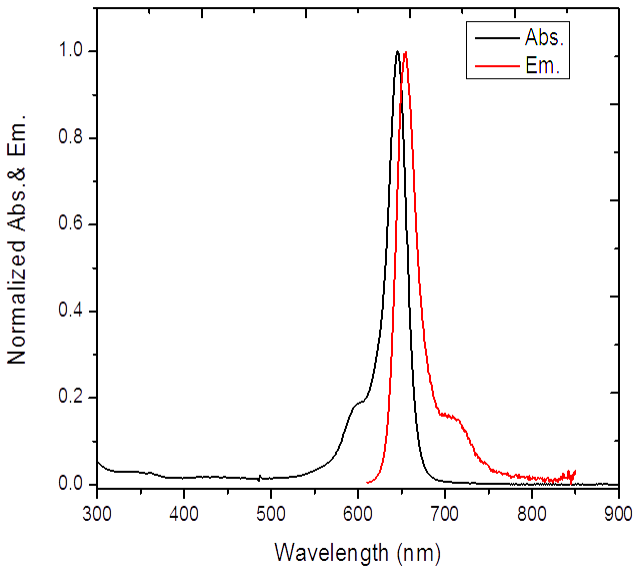

Figure 12. Absorption and emission spectrum of squaraine dye **(9')** in DMSO showing a λ_{max} = 645 nm for absorption and λ_{max} = 653 nm for emission.

3.3 Cytotoxicity (MTS) Assay Procedure

Cytotoxicity of the dyes SQ **(8')** and SQ **(9')** were tested using an MTS assay at various concentrations using human colorectal cancer (HCT-116) cells. The results obtained from these experiments are shown in **Figure 13** and **Figure 14**. The concentrations utilized for the cytotoxicity test of dye SQ **(8')** were 1, 5, 15, 25, 50 in µM. The viability of the cell line was maintained above 80%, at concentrations up to 25 µM, indicating good biocompatibility of the probe. The concentrations utilized for the cytotoxicity test of dye SQ **(9')** were 1.3, 3.1, 6.3, 12.5, 25, 50, 100 in µM. The same as for SQ **(8')**, the viability of the cell line incubated with SQ **(9')** was maintained above 80%, at concentrations up to 25 µM, indicating good biocompatibility of this probe as well.

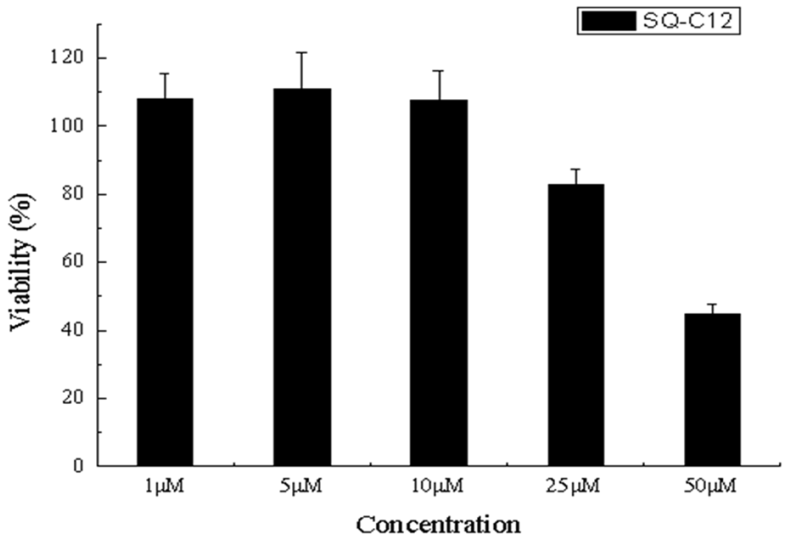

Figure 13. Cell viability test for squaraine dye **(8')**.

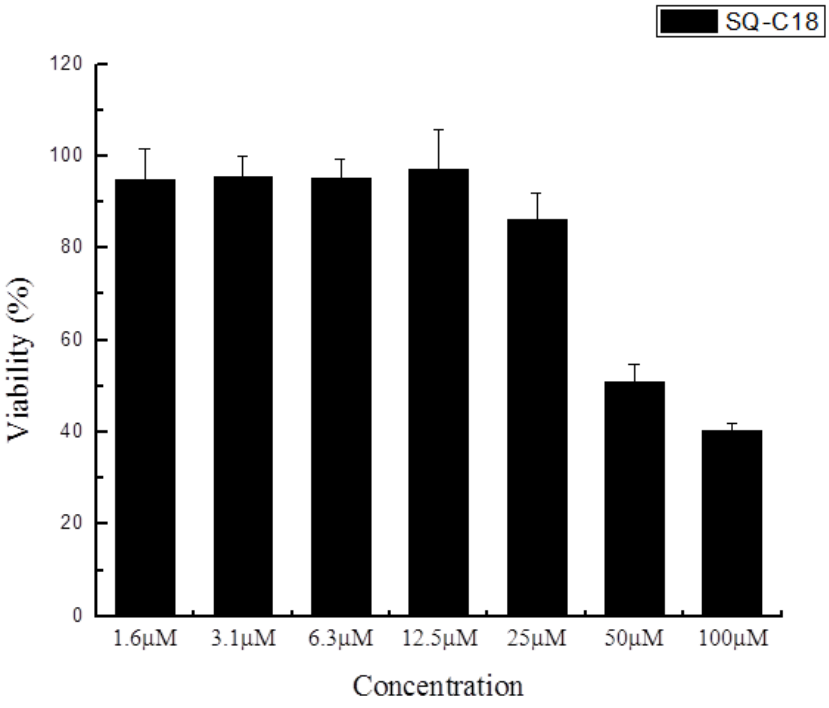

Figure 14. Cell viability test for squaraine dye **(9')**.

3.4 1PFM Cell Imaging: Colocalization Studies

The (HCT-116) human colorectal cancer cells were used in order to test the selectivity of squaraine dyes **(8')** and **(9')** and for the colocalization studies of the dyes. "In fluorescence microscopy, colocalization refers to an analysis method to characterize the degree of overlap between two different fluorescent labels, each having a separate emission wavelength, to determine if two different cellular "targets" are located in the same area."[16] Commercially available LysoTracker Red dye was used for the colocalization studies of dyes SQ **(8')** and SQ **(9')**. The LysoTracker Red probe is a fluorescent acidotropic probe for labeling and tracking acidic organelles in live cells, primarily lysosomes with high selectivity and effective labeling of living cells at nanomolar concentrations, although their two-photon action cross-section (which is the quantum yield multiply by the 2PA cross-section maximum of the dye) is very low (a value of 10 GM compared to the probes reported here with the lowest being above 1500 GM).[16] The fluorescence images were collected at different wavelengths, therefore the probability of cross-talk is low. As stated before, for squaraine dyes (**8')** and (**9')**, cells were excited at 633 nm and fluorescence images were collected in a range from 650 nm to 680 nm. For the LysoTracker Red probe, the cells were excited at 561 nm and fluorescence images were collected in a range from 580 nm to 630 nm. The images collected for both probes, as well as the differential interference contrast (DIC) image, are shown in **Figures 15** and **16**. Considering the overlay image of probe SQ **(8')** and SQ **(9')** with LysoTracker Red, it can be said that both are almost indistinguishable. Therefore, the probes show high specificity for binding in the lysosomes, as does the LysoTracker Red probe. Further tests can be done to confirm this conclusion, such as

calculating the colocalization coefficient, which indicates the relative degree of overlap between signals.

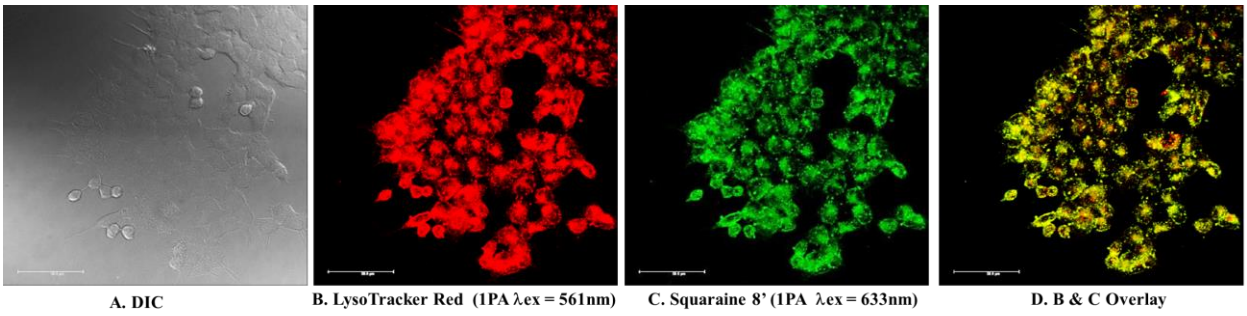

Figure 15. Colocalization images of HCT-116 cells with probe SQ **(8')** and LysoTracker Red. A water immersion 63x objective (HCX Pl APO CS 63.0×1.20 WATER UV) was used. A. DIC; B. One-photon confocal fluorescence image of LysoTracker Red; C. One-photon confocal fluorescence image of probe SQ **(8')** D. Overlay image of probe SQ **(8')** and LysoTracker Red.

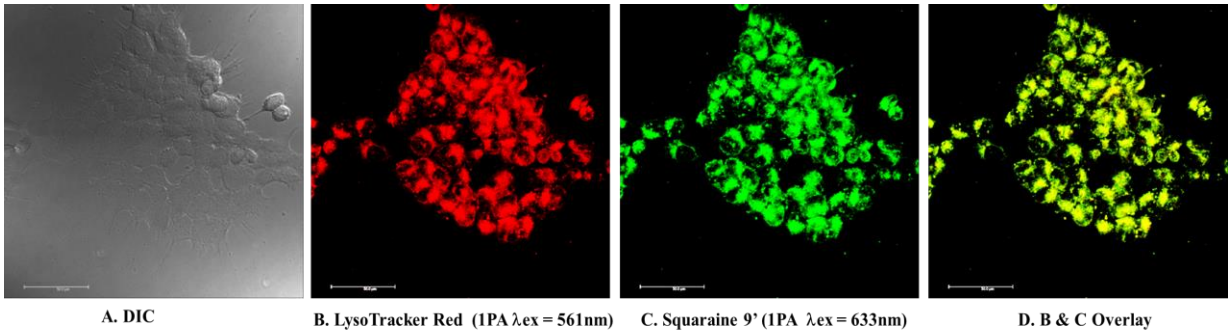

Figure 16. Colocalization images of HCT-116 cells with probe SQ **(9')** and LysoTracker Red. A water immersion 63x objective (HCX Pl APO CS 63.0×1.20 WATER UV) was used. A. DIC; B. One-photon confocal fluorescence image of LysoTracker Red; C. One-photon confocal fluorescence image of probe SQ **(9')** D. Overlay image of probe SQ **(9')** and LysoTracker Red.

3.5 2PFM Cell Imaging

Two-photon fluorescence microscopy images of the HCT-116 cells incubated with the probes SQ **(8')** and SQ **(9')** were obtained using the Leica TCS SP5 II microscope system, coupled to a tunable Coherent Chameleon Vision S (80 MHz, modelocked, 75 fs pulse width, tuned to 700 nm). The cells were excited at 800nm. An NDD detector (617/73) was used to collect two-photon fluorescence. As an example, a 2PFM image of HCT-116 cells incubated with both

probes is shown in **Figure 17C** and **Figure 18C**. For comparison, the DIC and the one-photon fluorescence images are also presented (**Figure 17A**, **17B**, **18A** and **18B**).The 2PFM image of the HCT-116 cells with the probe provides a higher resolution than conventional confocal imaging, supporting further investigations of this probes for bioimaging.[16]

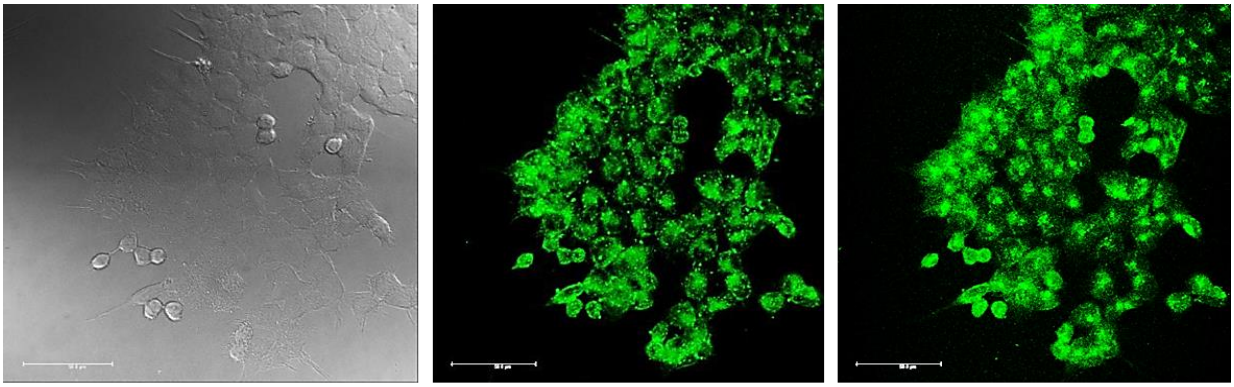

Figure 17. Images of HCT-116 cells coincubated with fluorescence probe SQ **(8')** taken with a water immersion 63x objective (HCX Pl APO CS 63.0×1.20 WATER UV). A. DIC; B. One-photon fluorescence image; C. 2PFM image excited at 800 nm, NDD detector (617/73).

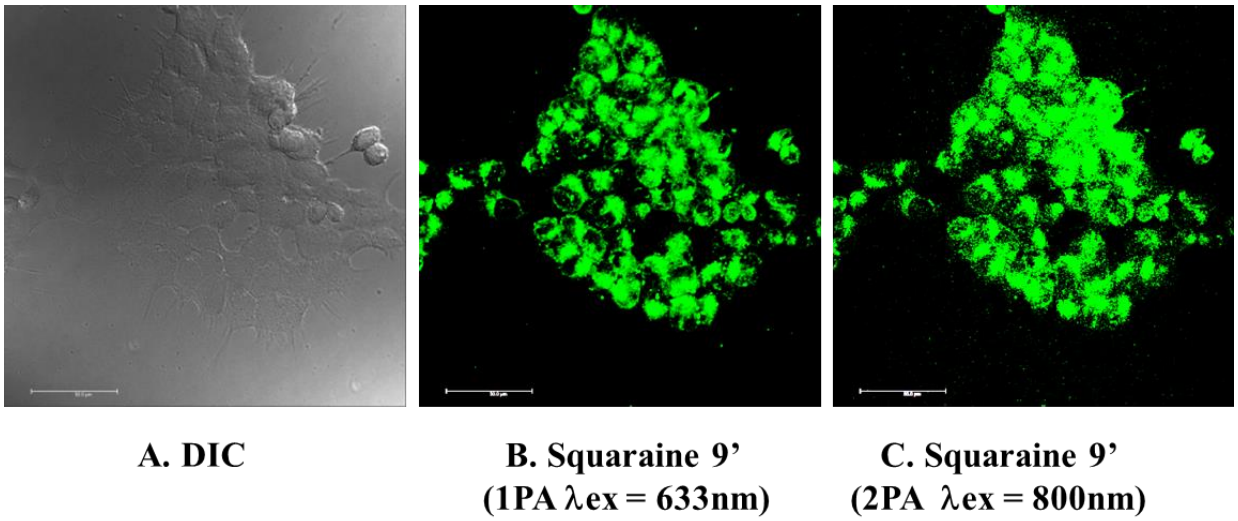

Figure 18. Images of HCT-116 cells coincubated with fluorescence probe SQ **(9')** taken with a water immersion 63x objective (HCX Pl APO CS 63.0×1.20 WATER UV). A. DIC; B. One-photon fluorescence image; C. 2PFM image excited at 800 nm, NDD detector (617/73).

CHAPTER 4: CONCLUSION

This study reports the successful synthesis and characterization of three near-infrared squaraine dyes. The applications of these dyes as 2PFM probes were evaluated. The dyes synthesized showed high two-photon absorption cross-sections, high quantum yields and photochemical stability. The Squaraine dyes **(8')** and **(9')** were incubated with human colorectal cancer (HCT-116) cells. The viability of the cell line was maintained above 80% at concentrations up to 25 μM, indicating good biocompatibility of the probes. Both probes were internalized by the cells resulting in high contrast fluorescence images. Using the LysoTracker Red probe, it is shown that the probes colocalized in the lysosomes.

For future work, the synthesis of specific dyes that are hydrophillic is considered. Introducing reactive groups to make bioconjugates for cancer cell targeting imaging will also be considered.

APPENDIX A:
^{1}H NMR AND ^{13}C NMR OF (4E,4'E)-2,2'-(5,5'-(1E,1'E)-2,2'-(9,9-DIETHYL-9H-FLUORENE-2,7-DIYL)BIS(ETHENE-2,1-DIYL)BIS(1-METHYL-1H-PYRROLE-5,2-DIYL))BIS(4-((3-ETHYL-1,1-DIMETHYL-1H-BENZO[E]INDOLIUM-2-YL)METHYLENE)-3-OXOCYCLOBUT-1-ENOLATE) (10)

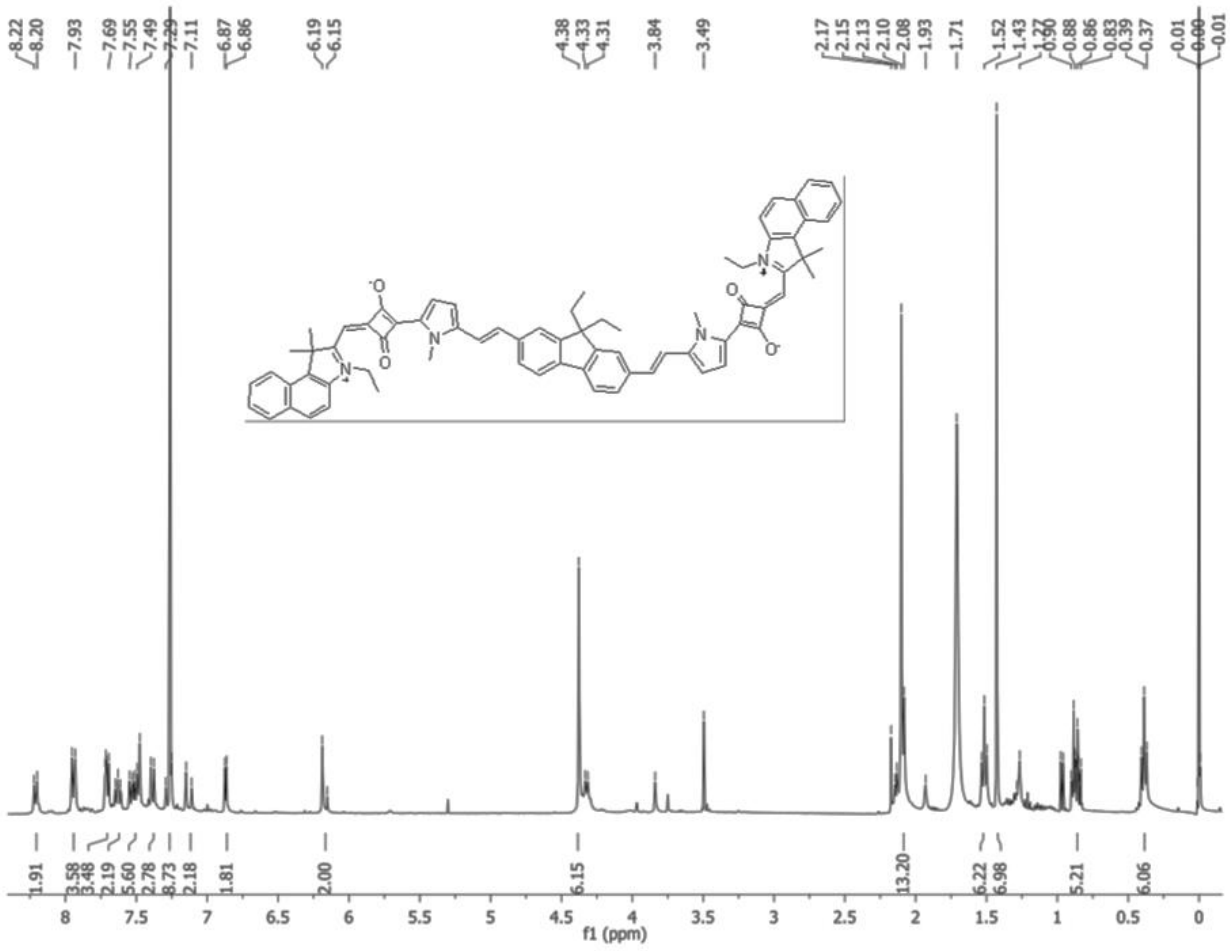

Figure 19. ^{1}H NMR spectrum of squaraine dye **(10)**.

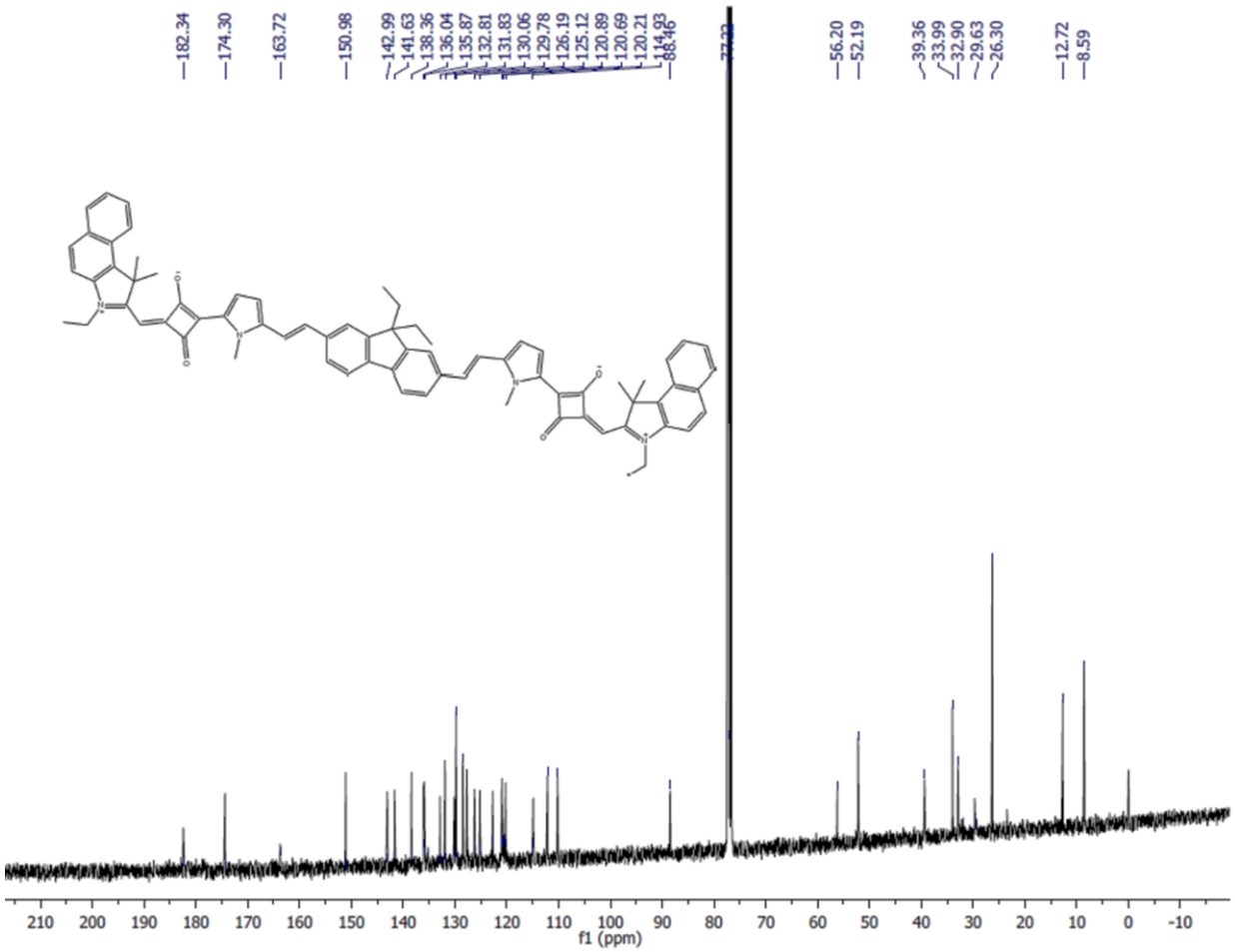

Figure 20. ^{13}C NMR spectrum of squaraine dye **(10)**.

APPENDIX B:
^{1}H-NMR AND ^{13}C-NMR OF (E)-2-((E)-(3,3-DIMETHYL-1-(3-SULFOPROPYL)INDOLIN-2-YLIDENE)METHYL)-4-((1-DODECYL-3,3-DIMETHYL-3H-INDOL-1-IUM-2-YL)METHYLENE)-3-OXOCYCLOBUT-1-ENOLATE (8')

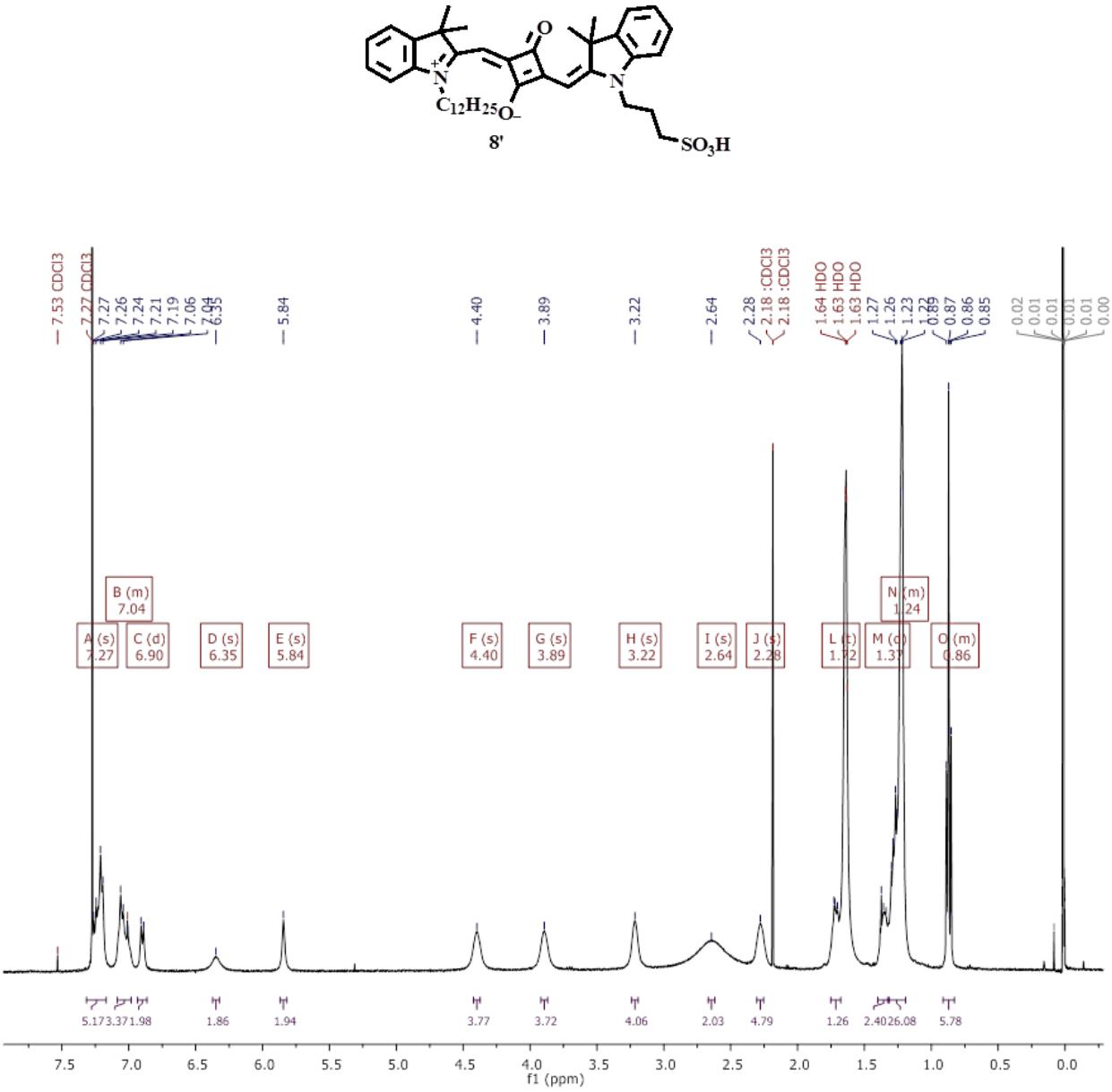

Figure 21. ^{1}H NMR spectrum of squaraine dye **(8')**.

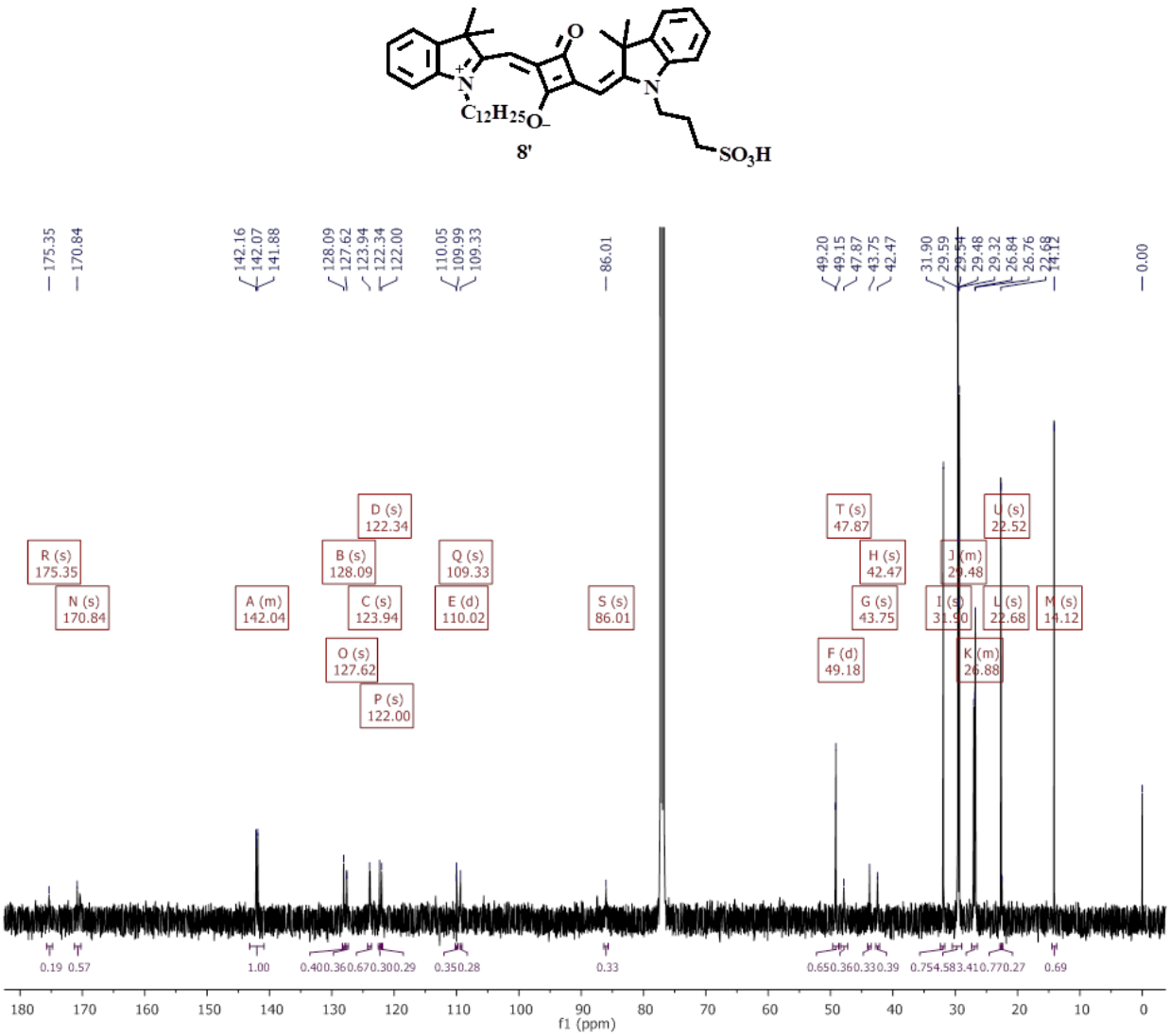

Figure 22. ^{13}C NMR spectrum of squaraine dye **(8')**.

APPENDIX C:
^{1}H NMR AND ^{13}C NMR OF (E)-2-((E)-(3,3-DIMETHYL-1-(3-SULFOPROPYL)INDOLIN-2-YLIDENE)METHYL)-4-((3,3-DIMETHYL-1-OCTADECYL-3H-INDOL-1-IUM-2-YL)METHYLENE)-3-OXOCYCLOBUT-1-ENOLATE (9')

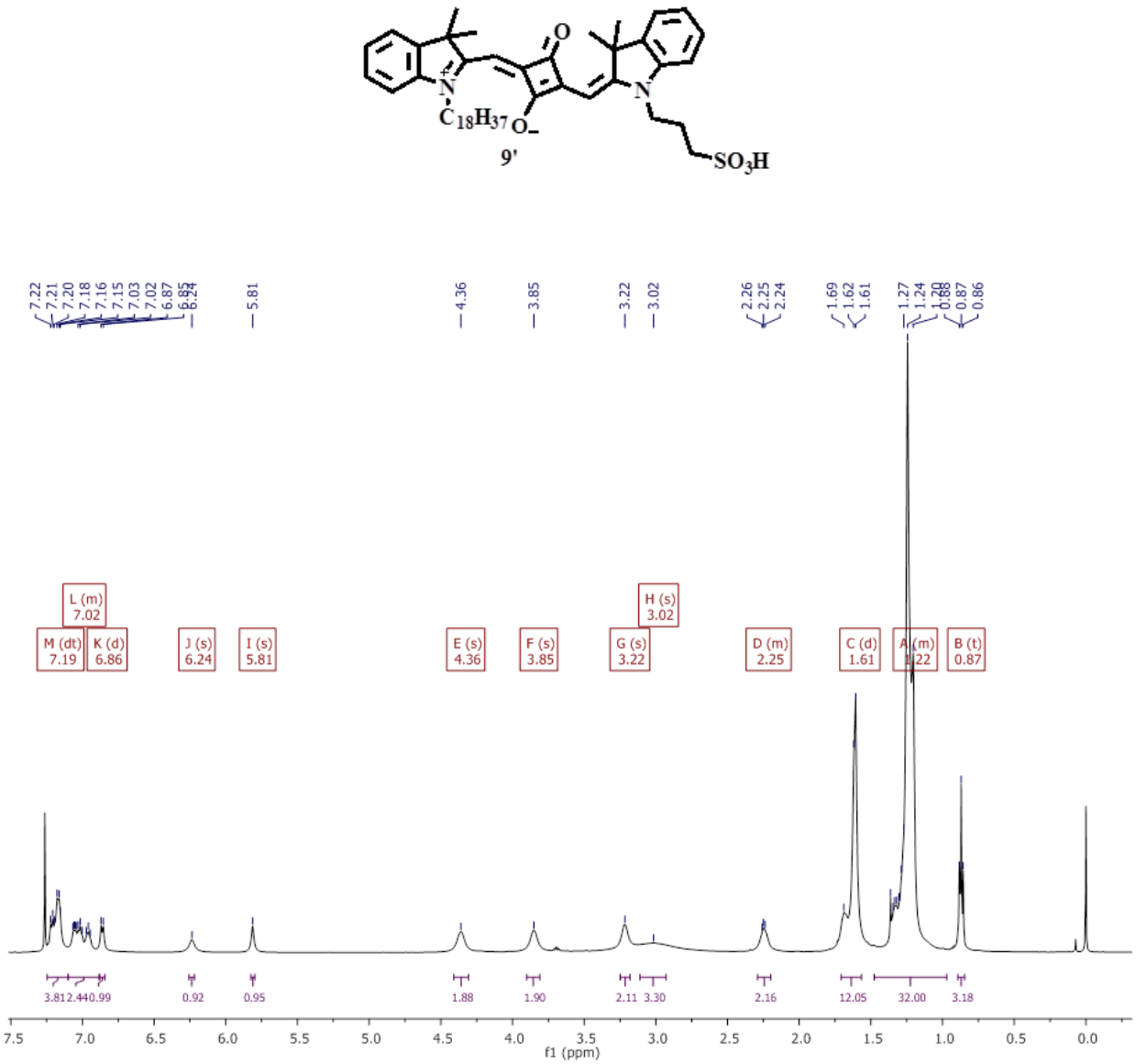

Figure 23. ^{1}H NMR spectrum of squaraine dye **(9')**.

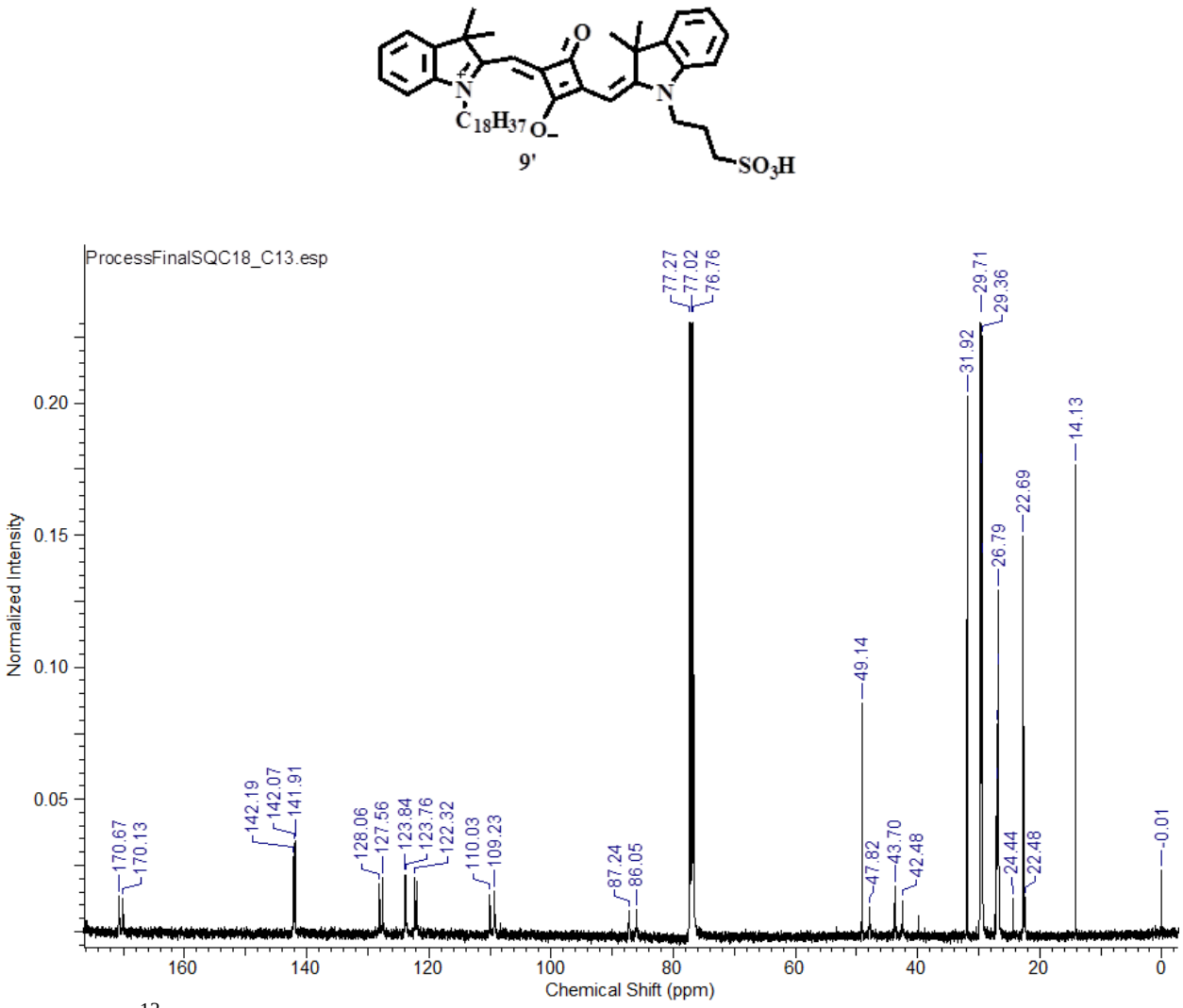

9'

Figure 24. ^{13}C NMR spectrum of squaraine dye **(9')**.

APPENDIX D:
HIGH RESOLUTION MASS SPECTRUM OF (4E,4'E)-2,2'-(5,5'-(1E,1'E)-2,2'-(9,9-DIETHYL-9H-FLUORENE-2,7-DIYL)BIS(ETHENE-2,1-DIYL)BIS(1-METHYL-1H-PYRROLE-5,2-DIYL))BIS(4-((3-ETHYL-1,1-DIMETHYL-1H-BENZO[E]INDOLIUM-2-YL)METHYLENE)-3-OXOCYCLOBUT-1-ENOLATE) (10)

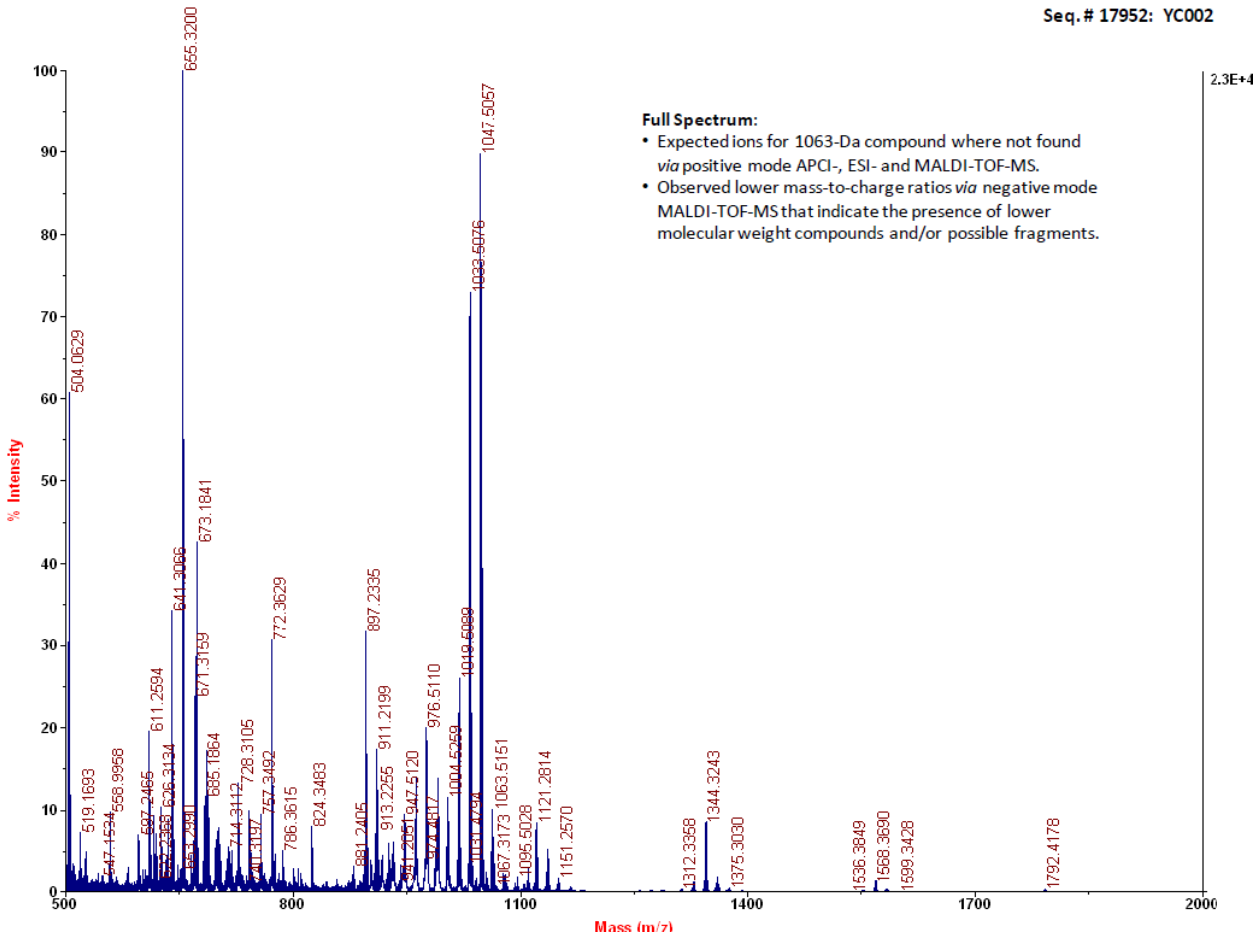

Figure 25. (Full Spectrum) HR Mass Spectrum of squaraine dye **(10)**.

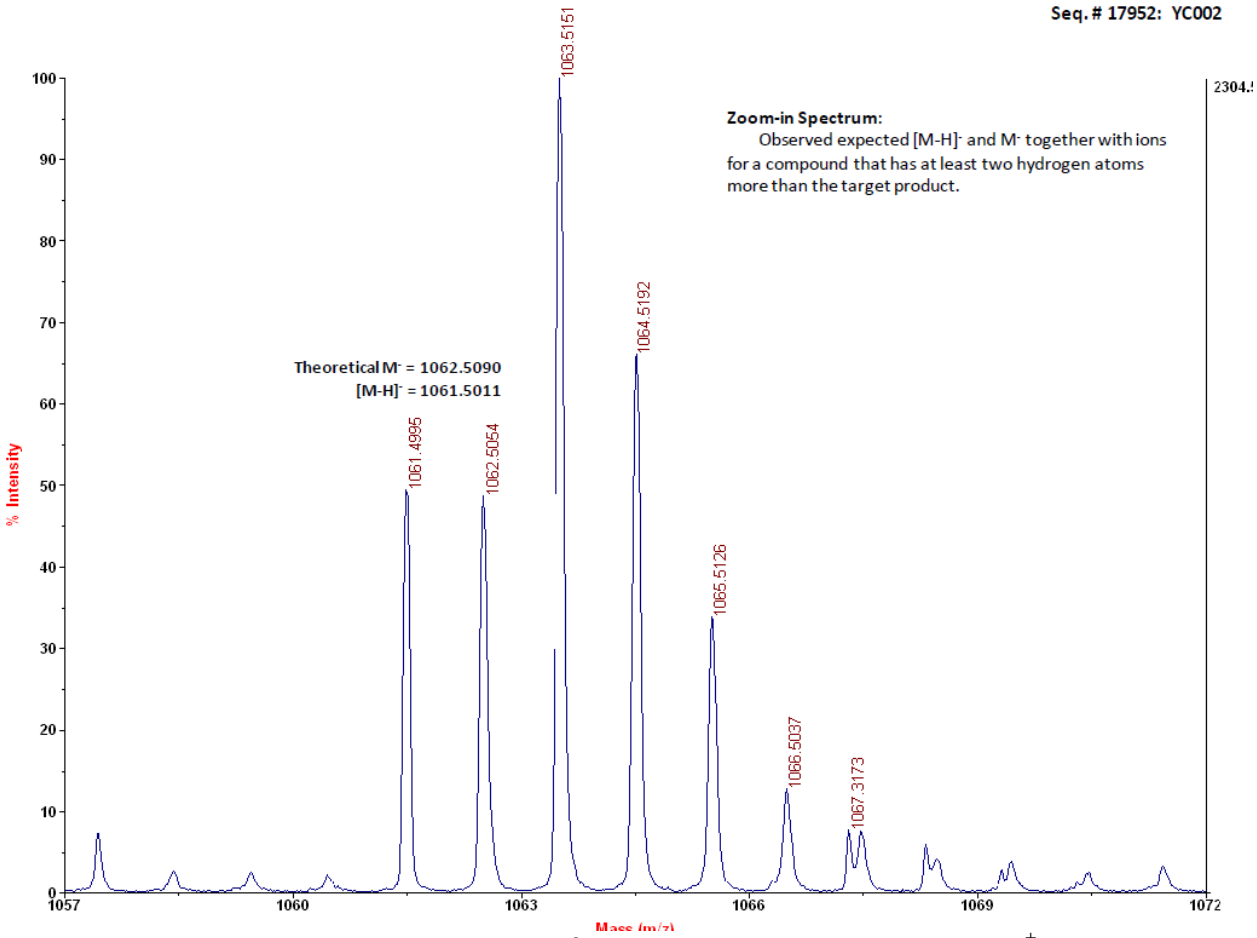

Figure 26. (Zoom-in) HR Mass Spectrum of squaraine dye **(10)**. Shows $[M+H]^+$

APPENDIX E:
HIGH RESOLUTION MASS SPECTRUM OF (E)-2-((E)-(3,3-DIMETHYL-1-(3-SULFOPROPYL)INDOLIN-2-YLIDENE)METHYL)-4-((1-DODECYL-3,3-DIMETHYL-3H-INDOL-1-IUM-2-YL)METHYLENE)-3-OXOCYCLOBUT-1-ENOLATE (8')

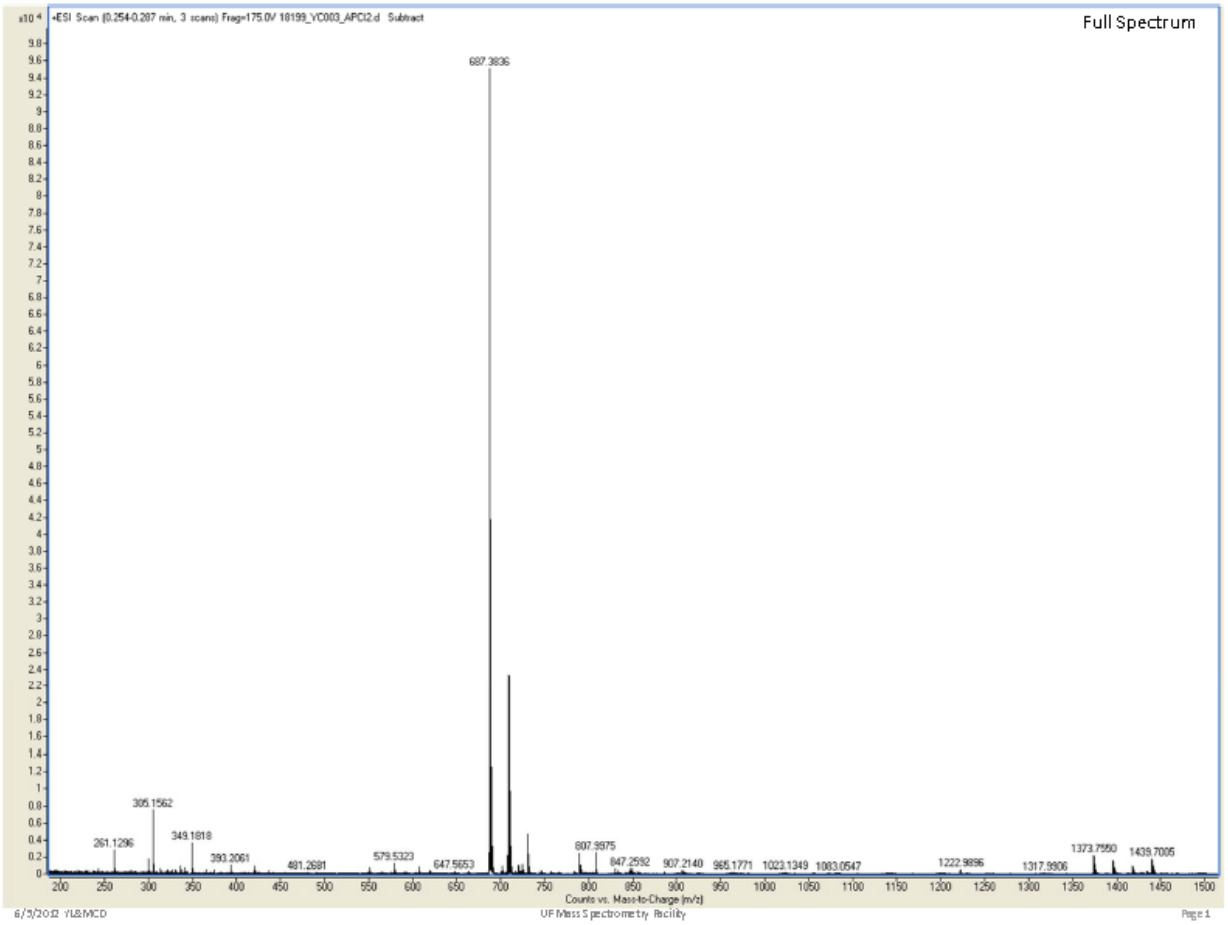

Figure 27. (Full Spectrum) HR Mass Spectrum squaraine dye **(8')**.

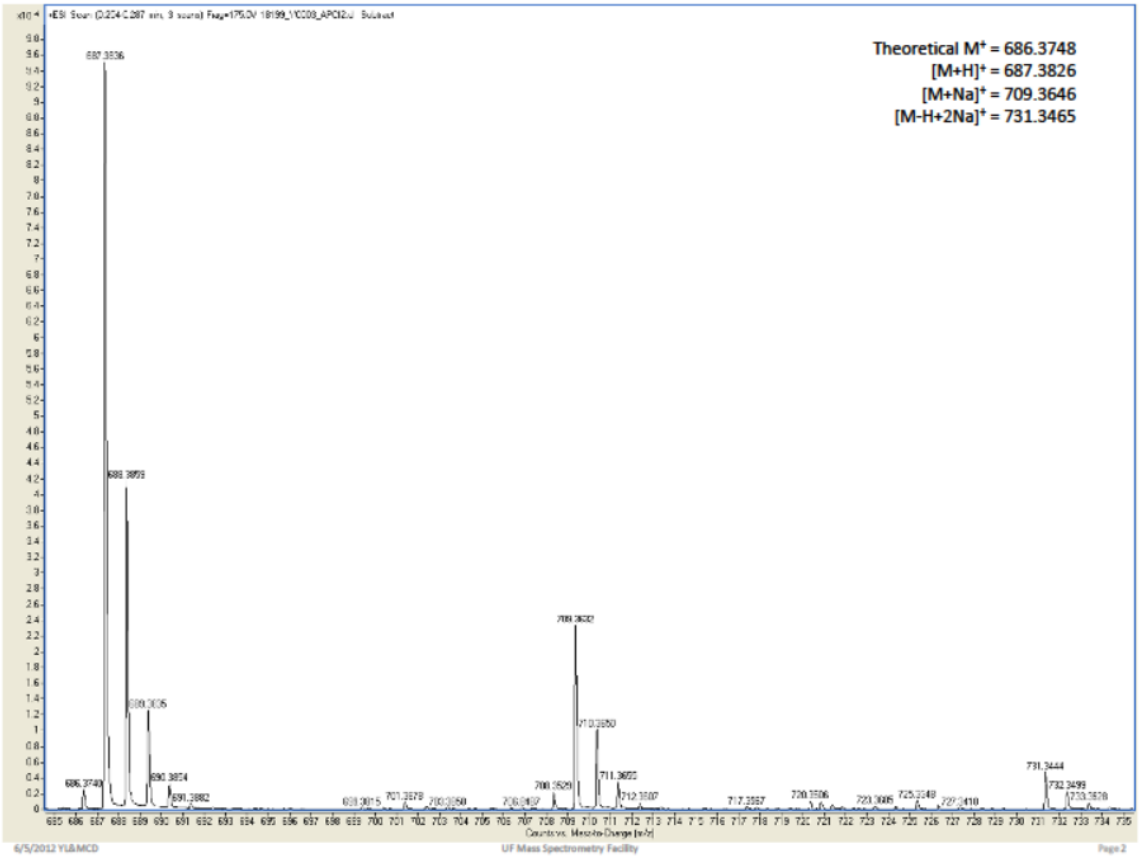

Figure 28. (Zoom-in) HR Mass Spectrum squaraine dye **(8')**. Shows $[M+Na]^+$

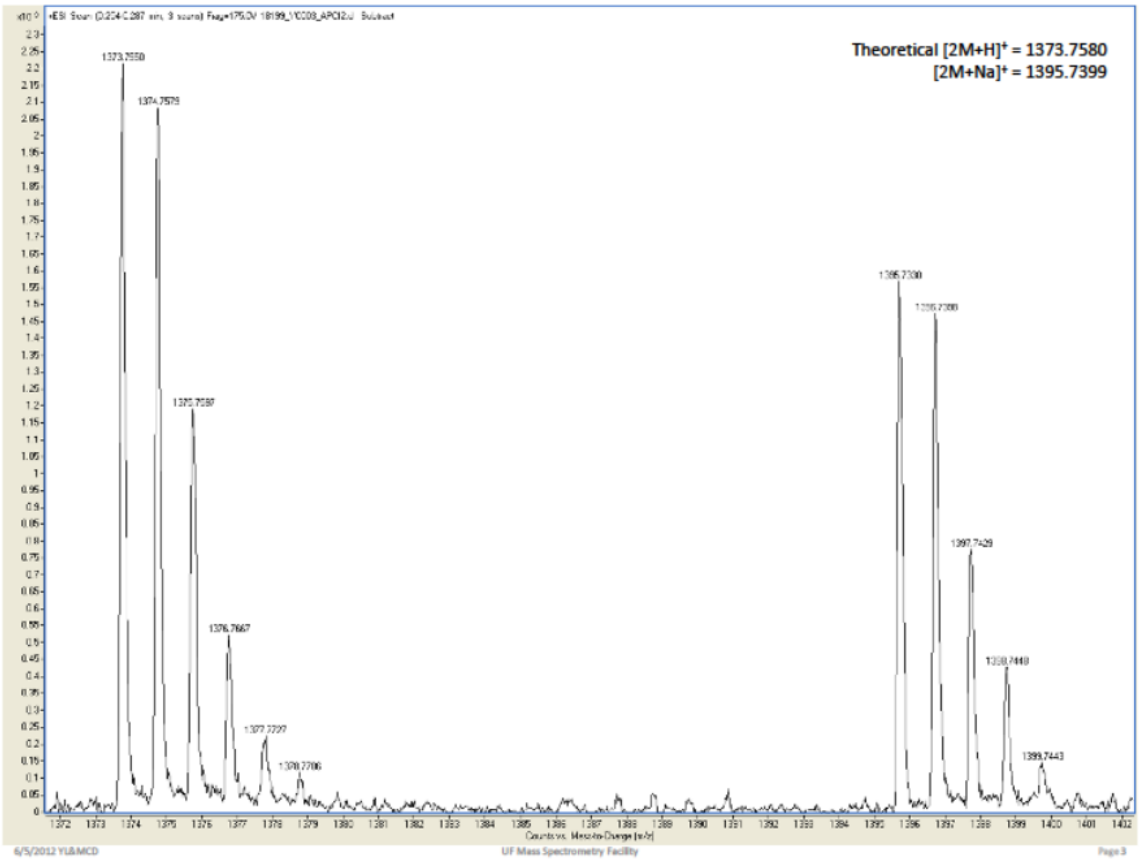

Figure 29. (Zoom-in) HR Mass Spectrum squaraine dye **(8')**. Shows $[2M+Na]^+$

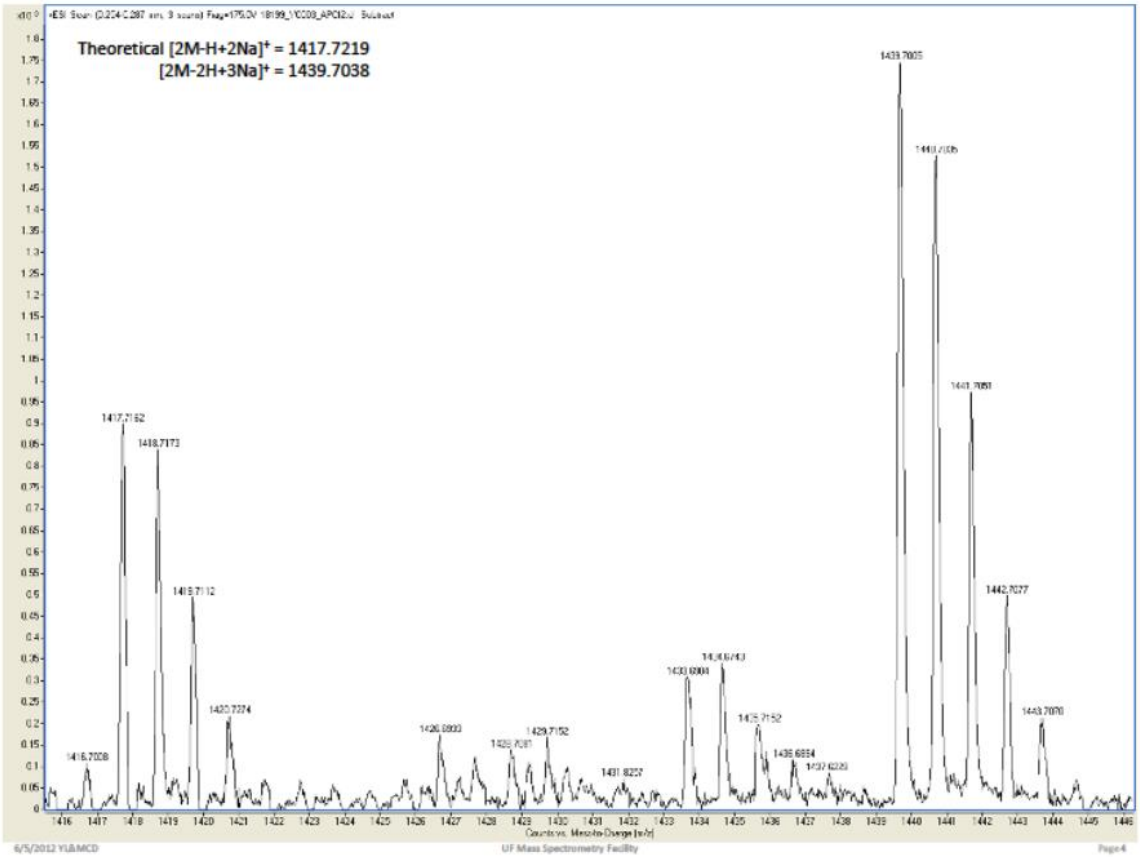

Figure 30. (Zoom-in) HR Mass Spectrum squaraine dye **(8').**Shows $[2M+2H+3Na]^+$

APPENDIX F:
HIGH RESOLUTION MASS SPECTRUM OF (E)-2-((E)-(3,3-DIMETHYL-1-(3-SULFOPROPYL)INDOLIN-2-YLIDENE)METHYL)-4-((3,3-DIMETHYL-1-OCTADECYL-3H-INDOL-1-IUM-2-YL)METHYLENE)-3-OXOCYCLOBUT-1-ENOLATE (9')

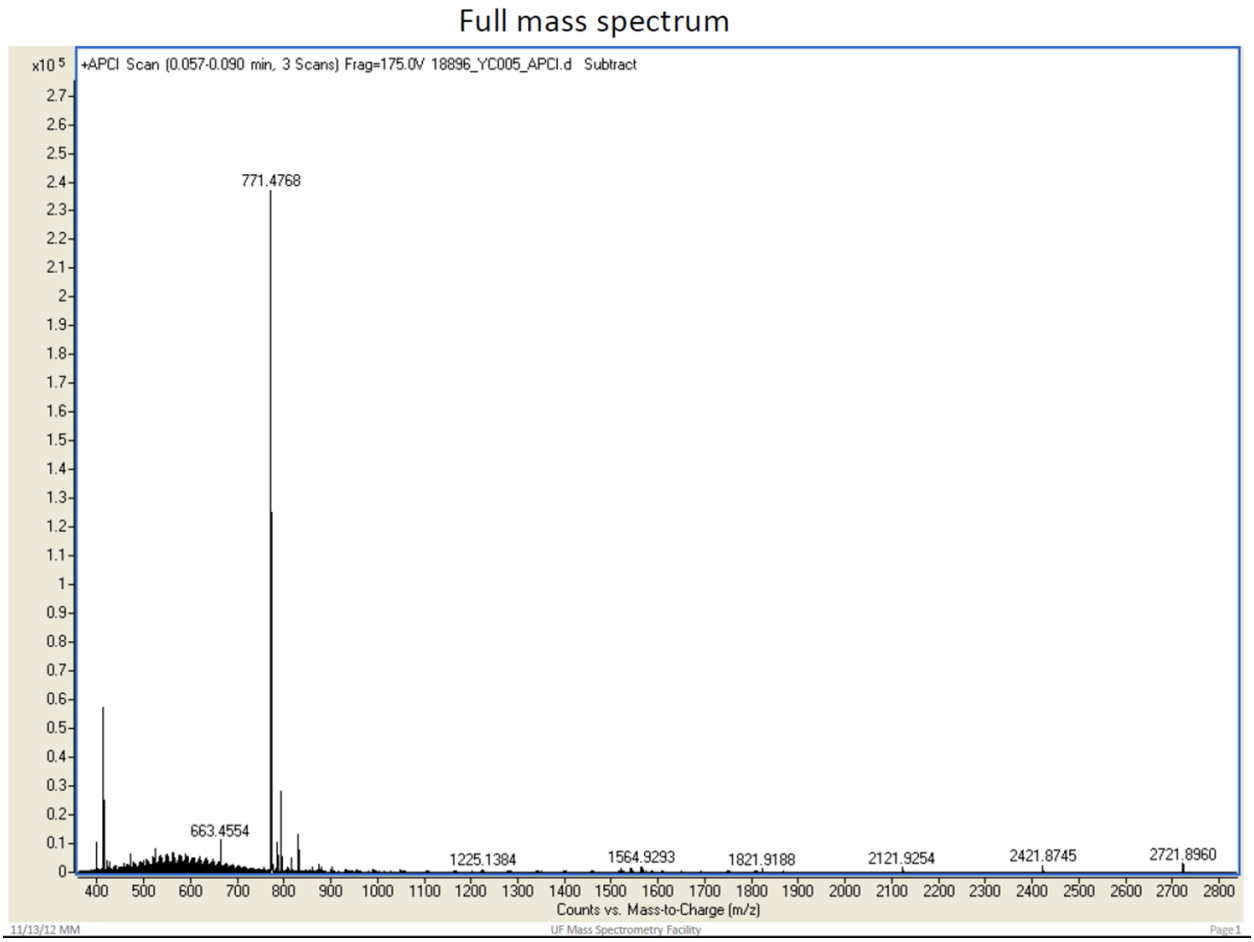

Figure 31. (Full Spectrum) HR Mass Spectrum squaraine dye **(9')**.

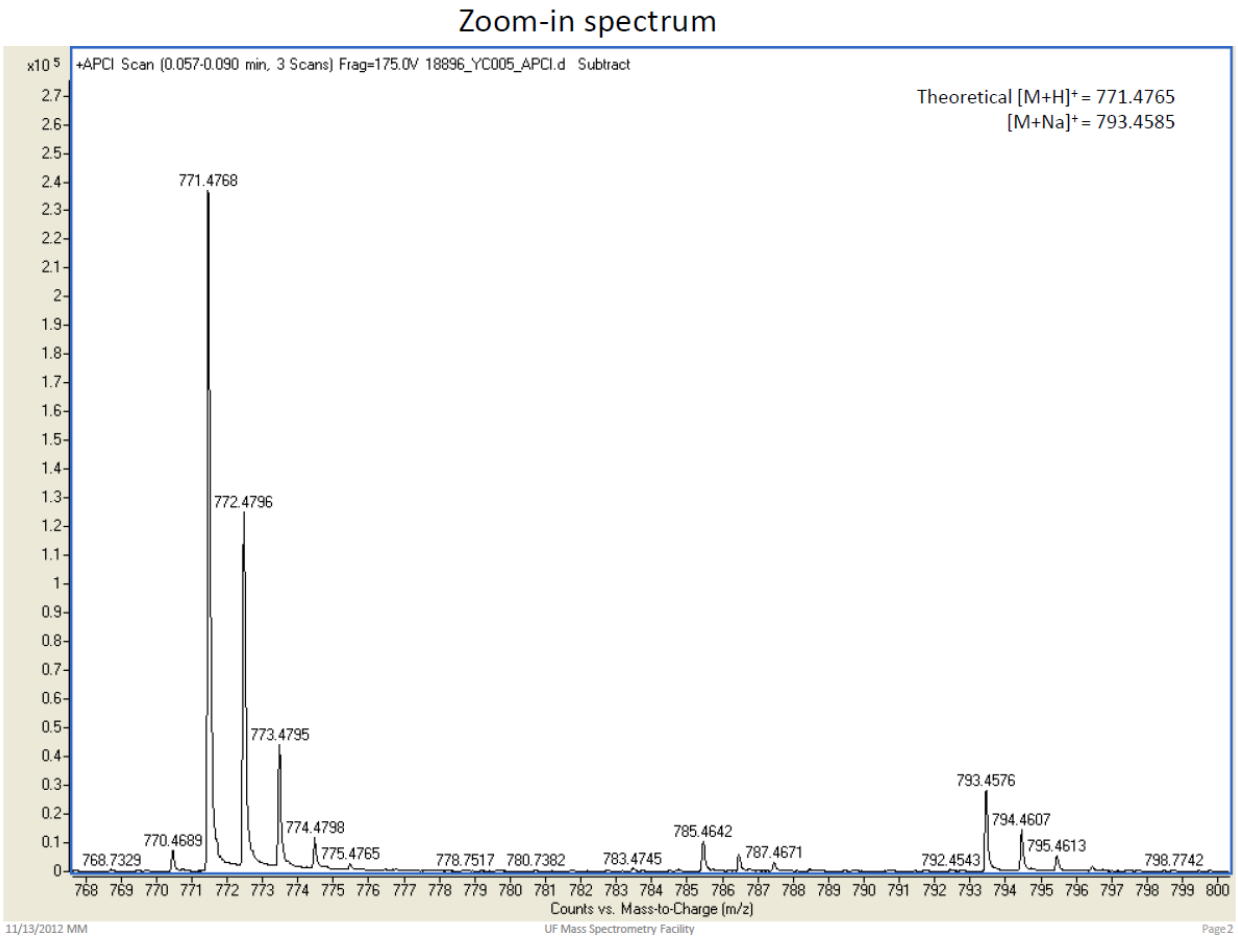

Figure 32. (Zoom-in) HR Mass Spectrum squaraine dye **(9')**. Shows $[M+Na]^+$

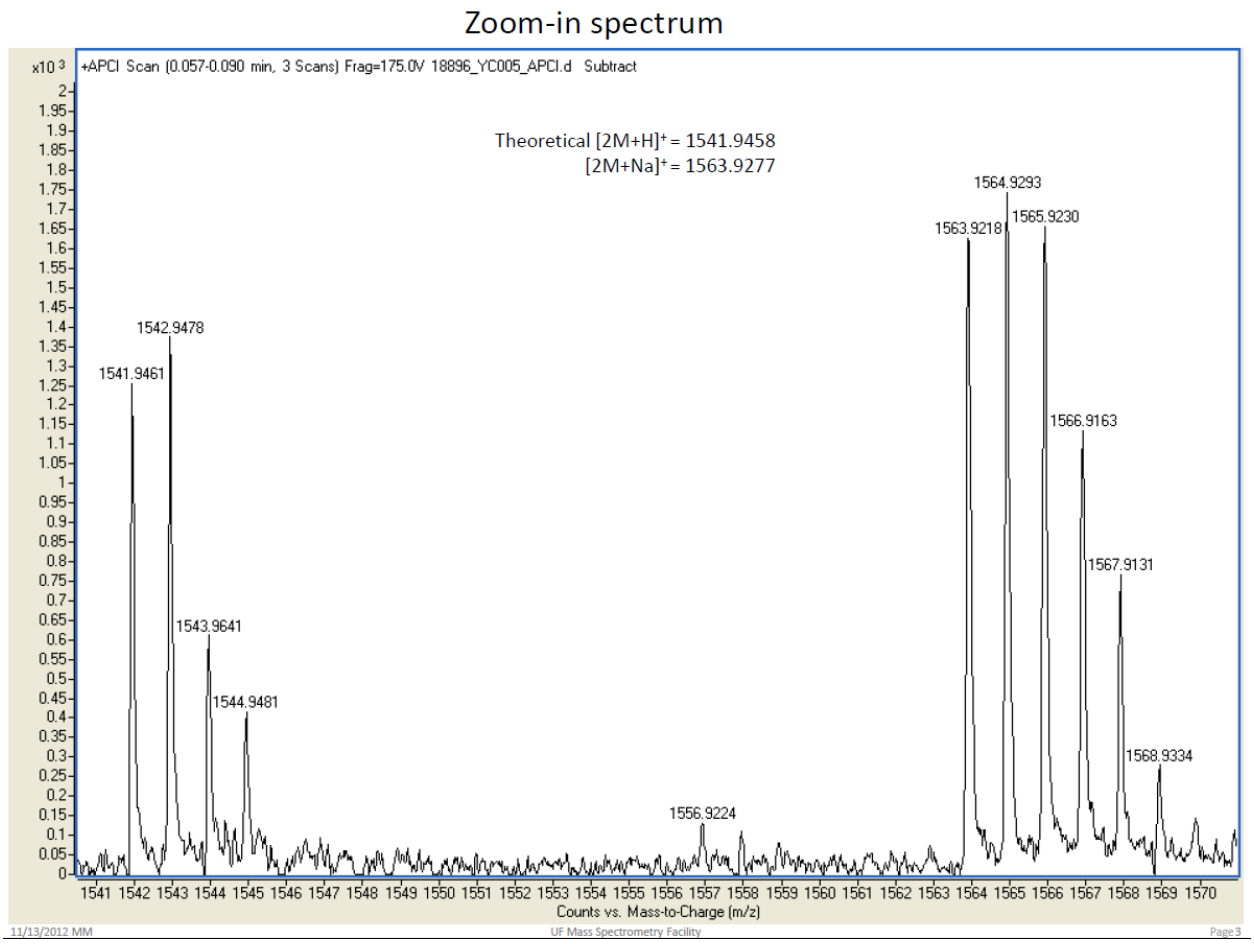

Figure 33. (Zoom-in) HR Mass Spectrum squaraine dye **(9')**. Shows $[2M+Na]^+$

REFERENCES

1. American Cancer Society. *Cancer Facts & Figures 2012*. Atlanta: American Cancer Society; **2012**.
2. Goetz, T. Wired. Why Early Detection Is the Best Way to Beat Cancer. http://www.wired.com/medtech/health/magazine/17-01/ff_cancer?currentPage=all (accessed October 18, 2012)
3. Joseph Thomas, *et. al.* "Synthesis and Biosensor Performance of a Near-IR Thiol-Reactive Fluorophore Based on Benzothiazolium Squaraine." *Bioconjugate Chem.* **2007**, *18*(6), 1841-1846.
4. Carlos Toro, Leonardo De Boni, Sheng Yao, Artem Masunov, Kevin Belfield, Florencio Hernandez. "Linear and Nonlinear Optical Characterization of a Monometric Symmetric Squaraine-Based Dye in Solution." The Journal of Chemical Physics **2009**, 130, 214504.
5. Belfield, Kevin D.; Yao, Sheng; Bondar. Mykhailo. "Organic Multiphoton Absorbing Materials and Devices." In *Introduction to Organic Electronic and Optoelectronic Materials and Devices*; Sun, Sam-Shajing; Dalton, Larry R. Ed.; CRC Press Taylor and Francis Group: Boca Raton, London, New York, **2008**; 574-575.
6. Jacques, S.L., Prahl, S.A., Oregon Graduate Institute, http://omlc.ogi.edu/classroom/ece532/class3/muaspectra.html, 1998; Anderson, R.R., Parrish, J.A., J. Invest Dermatol., 77, 13, **1981**.
7. Johnson, Ian D. and Michael W. Davidson. "Jablonski Energy Diagram". National High Magnetic Field Laboratory, 1800 East Paul Dirac Dr., The Florida State University, Tallahassee, Florida, 32310. **2004**, Retrieved from http://www.olympusmicro.com/primer/java/jablonski/jabintro/index.html
8. Herman, B., Lakowicz, J., Murphy, D., & Davidson, M. *Fluorescence excitation and emission fundamentals*. **2004,** Retrieved from http://olympusfluoview.com/theory/fluoro exciteemit.html
9. Mulligan, Sean J. and Brian A. MacVicar. "Two-Photon Fluorescence Microscopy: Basic Principles, Advantages, and Risks." **2007,** Retrieved from http://www.formatex.org/microscopy3/pdf/pp881-889.pdf
10. C. Xu. "Confocal and Two-Photon Microscopy; Foundations, Applications, and Advances." A. Diaspro, Ed. (Wiley-Liss, Inc., New York, **2002**, 75-99.
11. Göppert-Mayer, M., Elementary actions with two quantum leaps, Ann. Phys. 9, 273, **1931**.
12. Belfield, K. D.; Yao, S.; Bondar, M. V. "Two-photon Absorbing Photonic Materials: From Fundamentals to Applications" in Photoresponsive Polymers, *Advances in Polymer Science* **2008**, *213*, 97-156.

13. Ahn, H.; Yao, S.; Wang, X.; Belfield, K.D. “Near-Infrared-Emitting Squaraine Dyes with High 2PA Cross-Sections for Multiphoton Fluorescence Imaging.” *ACS Appl. Mater. Interfaces*. **2012**, *4*, 2847-2854.
14. Sheng Yao, Kevin D. Belfield. “Synthesis of Two-Photon Absorbing Unsymmetrical Branched Chromophores through Direct Tris(bromomethylation) of Fluorene.” *J. Org. Chem*. **2005**, *70*, 5126-5132.
15. Daniel E. Lynch, Andrew N. Kirkham, Mohammed Z. H. Chowdhury, Elizabeth S. Wane, John Heptinstall. “Water Soluble Squaraine Dyes for Use as Colorimetric Stains in Gel Electrophoresis.”*Dyes and Pigments*. **2012**, *94*(3), 393-402.
16. Sheng Yao, Hyo-Yang Ahn, Xuhua Wang, Jie Fu, Eric W. Van Stryland, David J. Hagan, and Kevin D. Belfield. “Donor-Acceptor-Donor Fluorene Derivatives for Two-Photon Fluorescence Lysosomal Imaging.” *J. Org. Chem*. **2010**, *75*, 3965-3974.